



OPEN DPP an extracellular matrix molecule induces Wnt5a mediated signaling to promote the differentiation of adult stem cells into odontogenic lineage

Yinghua Chen¹, Adrienn Petho¹, Amudha Ganapathy¹ & Anne George^{1,2}✉

Dentin phosphophoryn (DPP) an extracellular matrix protein activates Wnt signaling in DPSCs (dental pulp stem cells). Wnt/ β catenin signaling is essential for tooth development but the role of DPP-mediated Wnt5a signaling in odontogenesis is not well understood. Wnt5a is typically considered as a non-canonical Wnt ligand that elicits intracellular signals through association with a specific cohort of receptors and co-receptors in a cell and context-dependent manner. In this study, DPP facilitated the interaction of Wnt5a with Frizzled 5 and LRP6 to induce nuclear translocation of β -catenin. β -catenin has several nuclear binding partners that promote the activation of Wnt target genes responsible for odontogenic differentiation. Interestingly, steady increase in the expression of *Vangl2* receptor suggest planar cell polarity signaling during odontogenic differentiation. In vitro observations were further strengthened by the low expression levels of Wnt5a and β -catenin in the teeth of DSPP KO mice which exhibit impaired odontoblast differentiation and defective dentin mineralization. Together, this study suggests that the DPP-mediated Wnt5a signaling could be exploited as a therapeutic approach for the differentiation of dental pulp stem cells into functional odontoblasts and dentin regeneration.

Dentin is a unique, avascular mineralized connective tissue that forms the bulk of the tooth¹. It encloses a richly innervated and highly vascularized soft connective tissue the dental pulp. Dental pulp tissue contains mesenchymal stem/progenitor cells that possesses the properties of high proliferative potential, self-renewal and multi-lineage differentiation². Understanding the molecular mechanism that mediates the differentiation of adult-stem cells to regenerate the dentin-pulp complex is of significant interest in regenerative dental medicine^{3,4}. This process requires a fine balance between cell proliferation and differentiation. Differentiation of DPSCs to fully functional odontoblasts require selective activation of specific programs of gene expression. In vivo, these cells are believed to spontaneously differentiate when placed in the correct microenvironment and receive appropriate cues from the extracellular matrix.

Odontoblasts are neural-crest derived cells and are the principal cells that are responsible for the synthesis and secretion of the dentin matrix. Odontoblast polarization is a prerequisite and a fundamental process for tooth development and tubular dentin formation. They are metabolically active throughout the life of the tooth⁵ a requirement for tissue regeneration. Currently, there is sparse data available on the mechanism for odontoblast polarization.

The major extracellular matrix protein in the dentin matrix is a phosphoprotein that is rich in aspartic acid and serine-rich protein called dentin phosphophoryn (DPP)^{6,7}. DPP appears to be synthesized as a part of a larger compound protein, dentin sialophosphoprotein (DSPP)^{8,9}. DPP is a highly acidic protein which binds Ca^{2+} avidly and is thus linked to matrix mineralization¹⁰. Several in-vitro studies and the hypomineralized dentin phenotype of the DSPP-null mice confirm the crucial role DPP plays in the dentin matrix^{11–13}. We and others have shown that besides matrix mineralization, DPP functions as a signaling molecule^{14,15}. We have demonstrated that DPP stimulates intracellular calcium release in embryonic mesenchymal cells¹⁵. This depletion of calcium from the endoplasmic reticulum evokes a number of downstream responses.

¹Department of Oral Biology, University of Illinois Chicago, Chicago, IL 60612, USA. ²Department of Oral Biology, College of Dentistry, University of Illinois at Chicago, 801 S. Paulina St, Chicago, IL 60612, USA. ✉email: anneg@uic.edu

Several cell types secrete Wnts that bind cognate receptors on receiving cells to activate downstream signaling^{16,17}. Wnt signaling is an evolutionarily conserved signaling route and a study in the 1990s demonstrated that it's required for tooth formation¹⁸. During human and mice tooth development, specific Wnt signaling components have been shown to be expressed in the dental epithelium and mesenchyme^{19–21}. Animals models and functional studies indicate Wnt signaling effects regulate developing tooth formation and adult tooth homeostasis²⁰. Mutations in different Wnt signaling components is closely associated with syndromic and non-syndromic tooth agenesis, suggesting the importance of this signaling pathway as an attractive target for tooth disorders^{22,23}. During tooth development, Wnt5a is expressed predominantly in mesenchymal tissues from E11.5 (epithelial thickening) to E15.5 at the early bell stage^{18,24}. Wnt5a mRNA is extensively expressed in the developing odontoblasts and *Wnt5a*-deficient mice exhibit delayed odontoblast differentiation and the teeth are smaller and abnormally shaped²². The mammalian genome encodes 19 Wnt proteins and several receptors, however, the manner in which these components interact demonstrate dynamic and tightly controlled expression patterns in epithelial and mesenchymal cells during tooth development²³. However, there is little information regarding the mechanism by which Wnt5a is activated in the dental mesenchyme.

It is well-established that particular Wnt ligands can activate specific downstream signaling pathways depending on the available receptors. In canonical Wnt signaling, Wnt ligands (Wnt1, 2, 3,3a,7a,8a and 10b) bind cell surface receptors, Frizzled and low-density lipoprotein-receptor-related protein 5/6 which results in recruitment of Disheveled and Axin to the Fzd-Wnt-LRP5/6 complex. This leads to disassembly of the destruction complex leading to the nuclear accumulation of β -catenin and the activation of the transcription of β -catenin-target genes. Independent of the β catenin transcription, the non-canonical are the Wnt-Ca²⁺ pathway and the PCP pathway^{25,26}. Notable Wnt ligands in this pathway are Wnt4, Wnt5a and Wnt11 while ROR2 is a receptor.

Here we report the role of DPP in activating Wnt5a expression in dental pulp stem cells. Wnt5a like other Wnt ligands transduces its signal upon binding to different plasma membrane receptors or co-receptor complexes. The Wnt5a signaling cascades are diverse and it is capable of both inducing and repressing β -catenin signaling in vivo and is dependent on the cellular context^{27,28}. In this study, we first examined if DPP is the cue that promotes Wnt5a expression and induce odontogenic differentiation of DPSCs. Furthermore, we demonstrate that DPP stimulation is required for the expression of Frizzled5 and Lrp6 to activate WNT/ β -catenin signaling. Subsequently, the nuclear translocation of β -catenin, functions as a transcriptional regulator for odontogenic differentiation of DPSCs. We also demonstrate the expression of Ror2, a single-pass transmembrane protein with a tyrosine kinase domain and its interaction with Wnt5a. Identifying activators of the Wnt signaling pathway such as DPP could be therapeutically used to modulate the expression of Wnt target genes to aid dentin regeneration. These data provide a novel insight into harnessing the Wnt signaling pathway for therapeutic applications in regenerating the dentin-pulp complex.

Results

DPP and Wnt5a are secreted as an exosomal cargo by DPSCs

We first examined if Wnt5a and DPP were localized in the extracellular matrix (ECM). For this decellularized ECM from DPSCs were immunostained for Wnt5a and DPP. Results in Fig. 1A confirm the presence of DPP and Wnt5a in the ECM. Co-localization suggest that the two proteins are in close proximity and DPP might facilitate the interaction of Wnt5a with its cognate receptors. We had previously demonstrated that DPP was transported to the ECM in exosomes⁹. As Wnts are hydrophobic lipids, we examined their presence in the exosomal cargo. TEM imaging using immunogold labeled exosomes show the presence of DPP (20 nm, Black arrows) and Wnt5a (White arrows; 10 nm gold particles).

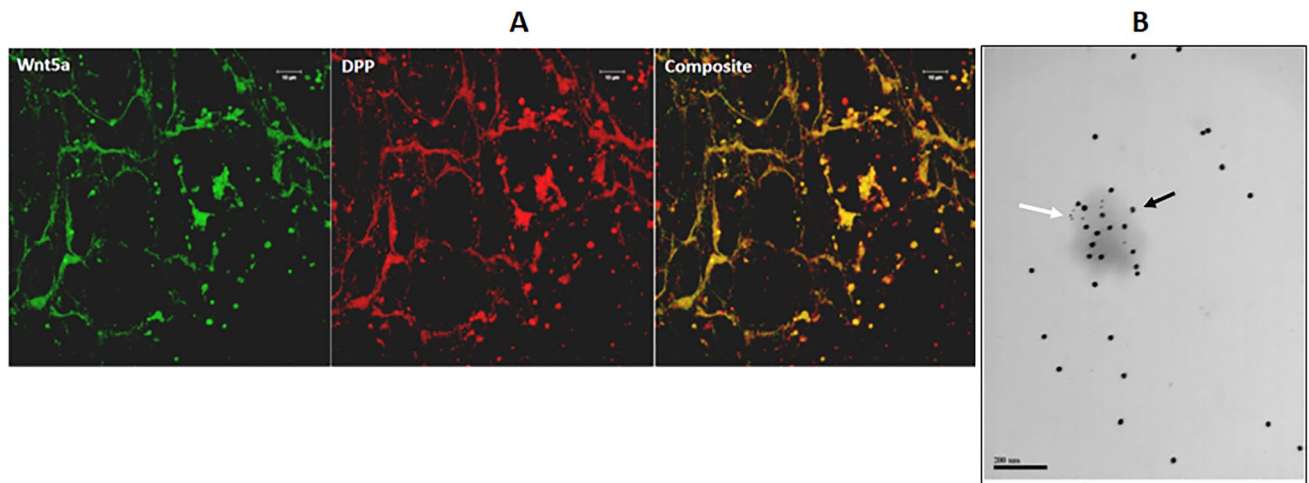


Figure 1. Wnt5a and DPP are present in the ECM of DPSCs and transported via Exosomes. (A) Representative confocal micrographs of ECM isolated from DPSCs immunostained for DPP (red) and Wnt5a (green). (B) Representative unstained TEM images of exosomes isolated from DPSCs showing the presence of DPP (black arrows; 20 nm gold particles) and Wnt5a (White arrows; 10 nm gold particles).

(10 nm, White arrows) Fig. 1B. These results suggest that both DPP and Wnt5a are present in the same exosome and reside in close proximity in the ECM.

To demonstrate induction of Wnt5a expression with DPP stimulation, total cellular proteins isolated from DPSCs cultured in growth media with DPP stimulation at various time points were subjected to Western blotting to examine the expression of Wnt5a. In Fig. 2A we show that Wnt5a protein expression increased continuously with DPP stimulation and higher expression levels were maintained until 72 h. However, pretreatment with NF- κ B pathway inhibitor TPCA-1 attenuated the increased expression of Wnt5a (Fig. 2A). To demonstrate DPP-mediated secretion of Wnt5a, we performed ELISA on the secretome of DPSCs stimulated with DPP and with and without the inhibitor TPCA-1. Results in (Fig. 2B) show basal levels of Wnt5a at time 0. At 15 and 30 min significant increase of Wnt5a was observed and higher levels after 30 min. TPCA-1 treatment abrogated the secretion of Wnt5a. These results confirmed that DPP stimulated the secretion of WNT5a and this activity was repressed by blocking NF- κ B signaling by TPCA-1.

Consistent with the protein expression data, *Wnt5a* gene transcripts also increased significantly to 4-fold when DPSCs were treated with DPP for 24 h when compared to 0 h (Fig. 2C). However, DPP-stimulated *Wnt5a* gene expression were repressed by pretreatment with NF- κ B inhibitors: TPCA-1 and JSH-23²⁹ (Fig. 2C).

In addition, *Wnt5a* promoter and NF- κ B reporter activities significantly increased with DPP treatment but pretreatment of DPSCs with TPCA-1 abolished these effects as revealed by luciferase assays (Fig. 2D). We then examined if the *Wnt5a* promoter contained an NF- κ B p65 binding consensus site (5'-GGGRNYYCC-3' where R: G/A; Y: C/T; N: A/C/G/T). Analysis revealed a DNA fragment containing the sequence TGGAAAGCCC which showed high sequence similarity to the structure of p50/p65 bound to DNA³⁰ To test the possibility that DPP activated *Wnt5a* gene expression by NF- κ B binding to the putative promoter elements, specific primer pairs (WNT_P420_81FW:-GGCCACAGTTGAGTAGTGGT-, WNT_P420_232RV:-TCCGTTTCCAACGTC CATCA-) flanking the TGGAAAGCCC region were designed and used to detect the DNA fragments in the

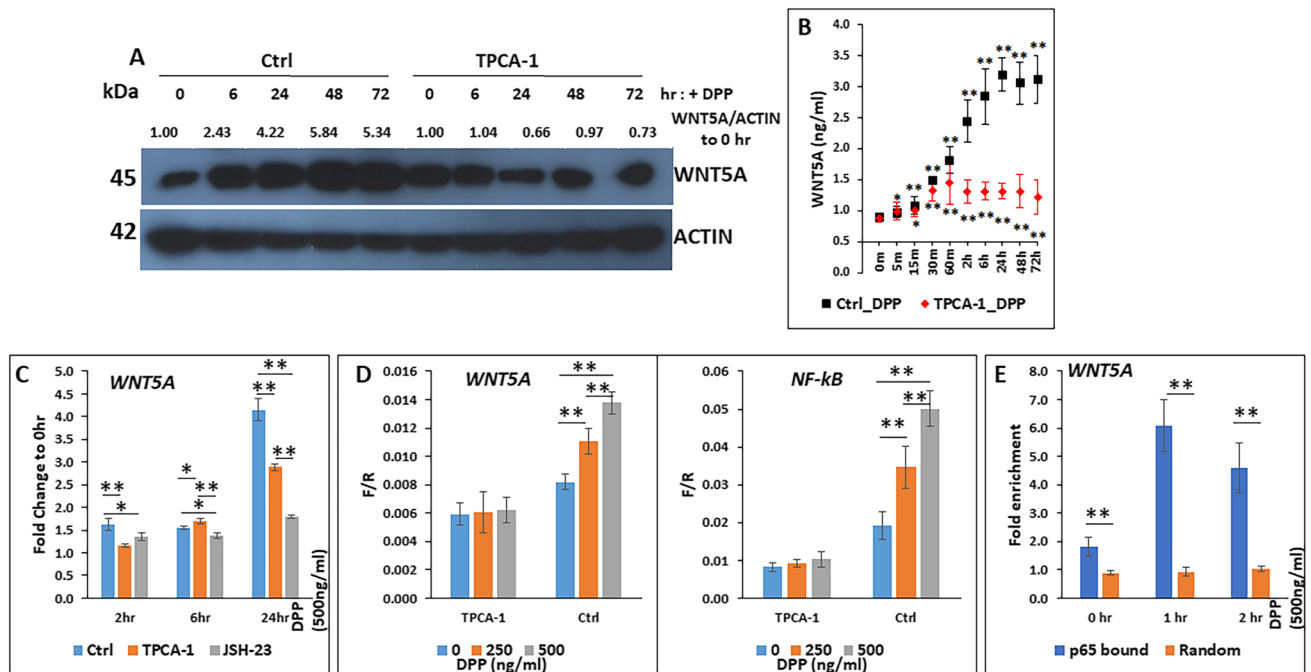


Figure 2. DPP stimulation of DPSCs activate Wnt5a signaling. **A.** DPSCs were treated with DPP (500ng/ml) in the presence and absence of the NF- κ B inhibitor TPCA-1. Stimulation was done at varying time points. Total levels of Wnt5a were examined by Western blotting. The densitometric ratios of Wnt5a normalized to actin are shown. **B.** DPSCs were treated with or without TPCA-1 for 1 h, followed by addition of DPP. The condition media was harvested at the times indicated. WNT5A concentration measured by direct ELISA, and mean and SD ($n = 8$) were plotted, * $p < 0.05$; ** $p < 0.01$. **C.** DPSCs were treated with DMSO (no inhibitor), TPCA-1 and JSH-23. Cells were stimulated with DPP at 500ng/ml for the indicated time points. Expression of Wnt5a gene expression levels were determined by RT-PCR. Fold change was obtained relative to 0 h. **D.** DPSCs were co-transfected with *Wnt5a* promoter luciferase plasmids or NF- κ B RE luciferase plasmids and treated with DMSO (no inhibitor) and TPCA-1 followed by stimulation with DPP at 0, 250, 500ng/ml. Luciferase activities were measured after 48 h. Mean values with standard deviation for Wnt5a and NF- κ B RE promoter activities were normalized to pCMV Renilla and transfection controls to Firefly/Renilla and plotted. Activity was abrogated when cells were treated with TPCA-1. **E.** ChIP assay was conducted with DPSCs treated with DPP for 0, 1 and 2 h as described in “Materials and Methods” using an anti-NF- κ B antibody and the immunoprecipitated DNA was analyzed by qPCR using primers for the NF- κ B binding site on the Wnt5a promoter. Mean values with standard deviation for fold enrichments of target DNA fragments, normalized to IgG antibody were plotted. * $p < 0.05$; ** $p < 0.01$.

ChIP products by RT-PCR. Primers amplifying random regions adjacent to the NF- κ B binding element were also synthesized (WNT_EX1_97FW: -CTCCATTCCTGGGCGCATC-. WNT_EX1_327RV: -CTTCATGGCG AGGGGAG-) and used as a negative control. To elucidate the DNA binding specificity, we conducted ChIP assay with an anti-p65 antibody using DPSCs treated with DPP for 1 h and 2 h. The enrichments of the DNA fragments flanking the putative NF- κ B binding site in Wnt5a gene promoter region were 1.80 fold at 0 h, and increased to 6.09 and 4.59 fold at 1 h, and 2 h respectively. However, there were no enrichments with non-specific primers of random DNA fragments: 0.89, 0.92, and 1.04 fold at 0, 1, and 2 h, respectively (Fig. 2E).

DPP stimulation induces Wnt5a dependent stabilization and subsequent nuclear translocation of β -catenin

Activation of β -catenin is the central effector of canonical Wnt pathway. However, Wnt5a has been reported to activate β -catenin dependent and independent signaling²⁷. Canonical Wnt signaling orchestrates a response through nuclear accumulation of β -catenin in the cell population as seen in osteoblastogenesis³¹. Therefore, we analyzed if DPP-mediated Wnt5a activation could orchestrate the translocation of β -catenin to the nucleus. Subcellular fractionation and Western blotting results in Fig. 3A show increased nuclear expression of β -catenin with DPP stimulation and reduced expression in the cytoplasmic fraction. In the nuclear fraction, there was no detectable contamination from the cytoplasm as indicated by the absence of the cytoplasmic protein tubulin.

In order to study the endogenous β -Catenin expression and localization we performed confocal immunofluorescence microscopy. For this cell treated with DPP for 0 m, 5 m, 15 m, 30 m, and 60 m, were fixed and permeabilized and detected for nuclear β -Catenin. Accumulation of nuclear localization of β -Catenin was detected as early as 5 min of DPP stimulation and peaked at 15 min (Fig. 3B). Interestingly, pretreatment with TPCA-1 to repress Wnt5a expression, activated by DPP stimulation, show reduced levels of nuclear β -Catenin (Fig. 3C). Disrupting the interaction between Wnt5a and its receptor(s) by pretreatment with Wnt5a antagonist Box5, show reduced levels of nuclear translocation of β -catenin with DPP stimulation (Fig. 3D). In addition, nuclear translocation of β -catenin was not detected in DPSC/Wnt5a- KO cells regardless of DPP treatment (Fig. 3E). Nuclear translocation of β -catenin was also observed with recombinant Wnt5a treatment (Fig. 3F) and with agonist antibody of FZD and LRP6, PF-L6 which served as a positive control (Fig. 3G). Collectively, these studies establish that DPP mediated Wnt5a activation promotes the nuclear translocation of β -catenin and their translocation could be aborted in the absence of Wnt5a.

DPP stimulation activates Wnt/ β -catenin signaling route to regulate the expression of Wnt target genes

Previously, we have demonstrated that DPP stimulation could upregulate the gene expression of key odontogenic genes such as *RUNX2*, *OSX*, *ALP*, and *OCN*²⁹. Therefore, we analyzed if the mechanism that increased these transcripts were regulated by Wnt/ β -catenin signaling. RT-PCR analysis performed on DPSCs treated with inhibitors Box5, iCRT14 drug³² and DMSO (no inhibitor) for 1 h and then stimulated with DPP for 0 h, 2 h, 6 h, and 24 h were used to assess the gene expression pattern. Results in Fig. 4(A-E) showed that in the absence of the inhibitors, DPP treated DPSCs effectively showed increased expressions of *RUNX2*, *OSX*, *ALP*, *OCN* and *DMPI*. In contrast, pretreatment of DPSCs with Wnt/ β -catenin pathway inhibitors and DPP stimulation, resulted in decreased gene expression (Fig. 4A-E).

DPP stimulation activates specific Wnt ligand receptors while treatment with Wnt5a antagonist abrogated their expression

Availability of specific Wnt receptors is a key factor in deciding the specificity and the strength on the expression of the downstream targets of Wnt signaling. Results in Fig. 5A show that DPP significantly induced/enhanced protein expressions of FZD5, LRP6, and ROR2, but only slight increase in expression of FZD6 and LRP5 was observed. In contrast, pretreatment with Wnt5a antagonist Box5 reduced the expression of the receptors to varying degrees even after DPP stimulation. Reduced expression was prominent with FZD5, LRP5, LRP6 and ROR2 at 500 μ M of Box5 (Fig. 5B).

DPP stimulation promotes colocalization of Wnt5a with receptors signaling through both canonical and noncanonical signaling pathway

Wnt5a signaling is activated in response to DPP stimulation resulting in the Wnt ligand binding to its receptor (s). We monitored the endogenous expression and localization of Wnt5A and its receptor's after DPSC's were stimulated with DPP for 0 m, 5 m, 15 m, 30 m, and 60 m. Addition of DPP increased puncta- formation of Wnt5a-FZD5 (Fig. 6A), Wnt5a-LRP6 (Fig. 6C), Wnt5a-ROR2 (Fig. 6E). Maximum co-localization signals were observed at 15 m for Wnt5a-FZD5, 30 m for Wnt5a-LRP6, and 30 m for Wnt5a-Ror2 as indicated by Pearson's coefficient. In contrast, similar experiments performed with DPSC/Wnt5a KO cells showed no puncta formation as no Wnt5a protein expression was detected (Fig. 6B, D and F).

DPP stimulation promotes the binding of Wnt5a to Ror2 receptor at the cell membrane and subsequent internalization

Interaction between Ror2 and DPP was analyzed by total internal reflection fluorescence (TIRF) microscopy using Wnt5a-EGFP and Ror2-mCherry transfected HEK293T cells due to its high efficiency of transfection. (Fig. 6G). Distribution of Wnt5a (green) and Ror2 (red) were distinctly observed on the membrane surface in unstimulated cells. Upon addition of 500ng/ml DPP, the presence of Wnt5a and Ror2 decreased in the TIRF zone, suggesting that Wnt5a binds to Ror2 on the cell surface and is internalized with DPP stimulation. Interestingly, increased expression of *Vangl1* & *Vangl2* (*Van Gogh*), components of the planar cell polarity (PCP) signaling

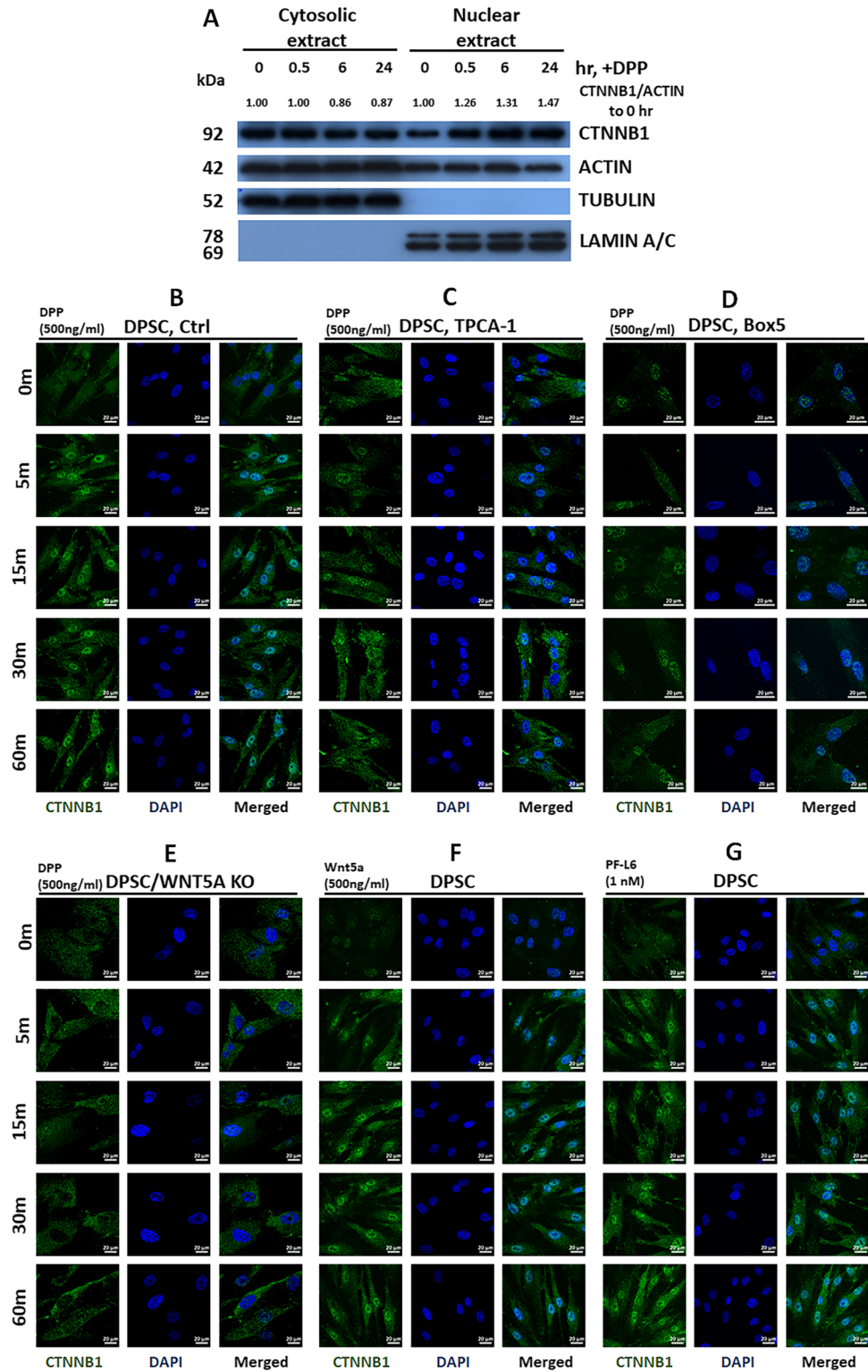


Figure 3. DPP stimulation of DPSCs promote nuclear translocation of β -catenin by activating WNT5A. **A.** Cell fractionation of DPSCs treated with DPP for 0, 0.5, 6 and 24 h were performed. Immunoblotting using anti- β catenin antibody showed higher amounts of nuclear accumulation as shown by the β -catenin to actin ratio. Tubulin and Lamin A/C were used as controls to demonstrate the purity of cytoplasmic and nuclear extracts. **B to E.** Immunofluorescence images of DPSC or DPSC/Wnt5a-KO cells treated with DPP for 0, 5, 15, 30 and 60 min. Images were also acquired in the presence of inhibitors TPCA-1& Box5 with DPP stimulation. Note the low levels of nuclear β -catenin in the presence of inhibitors and in Wnt5a-silenced cells. **F and G.** Immunofluorescence images of DPSCs treated with Wnt5a (positive control) and PF-L6 (positive control for 0,5,15, 30 and 60 min to demonstrate nuclear translocation of β -catenin .DAPI (blue) stains the nucleus. Scale bar 20 μ m.

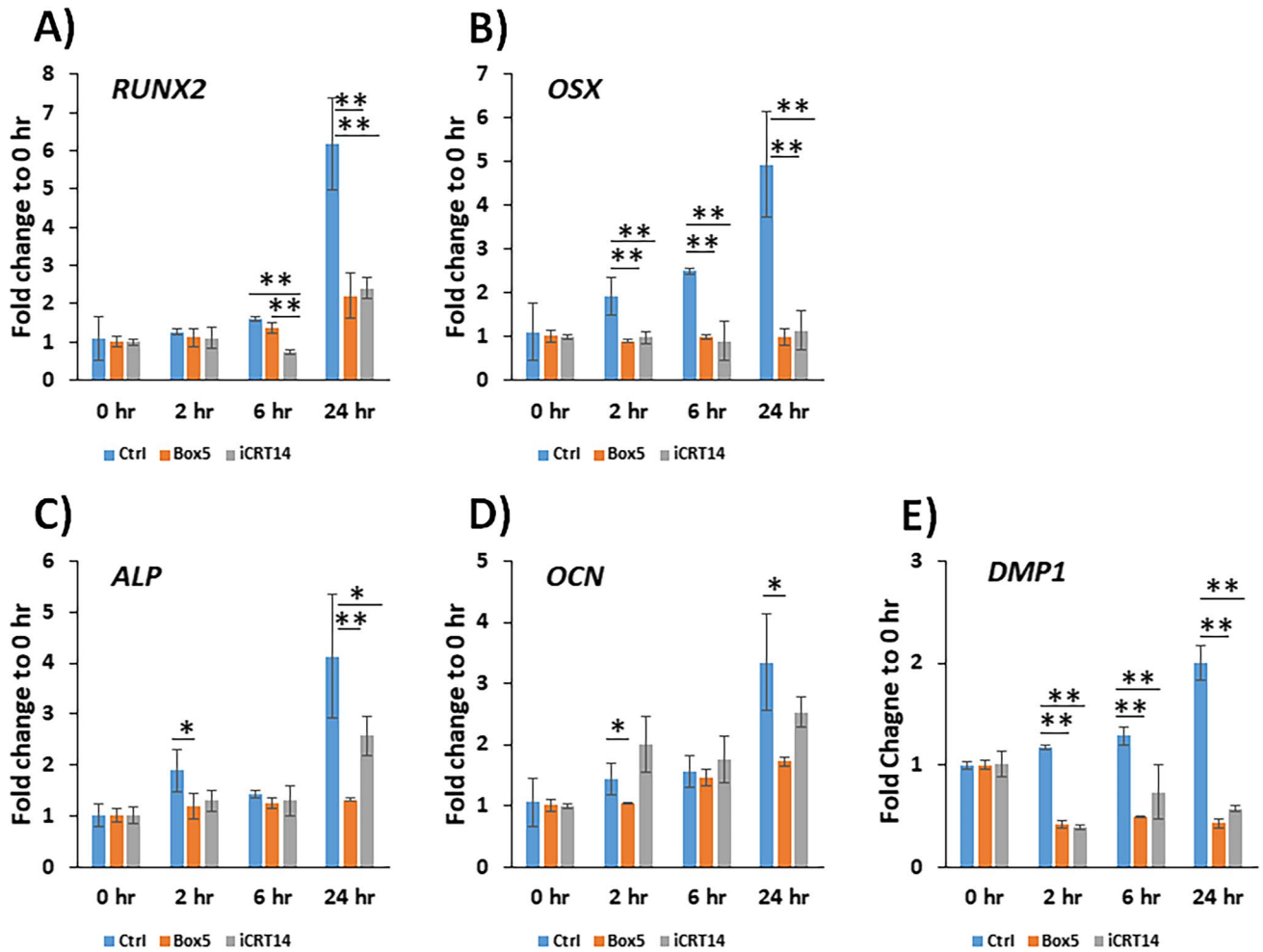


Figure 4. DPP activates the expression of odontogenic markers through Wnt5a/ β -catenin signaling and abrogates their expression in the presence of Wnt5a/ β -catenin pathway inhibitors. DPSCs were cultured under growth conditions and were treated with DMSO; with Box5 or iCRT14. In all conditions cells were stimulated with 500ng/ml DPP and cultured for 0, 2, 6 and 24 h. Total RNA was isolated and quantitative RT-PCR analysis performed. Fold changes were obtained relative to 0 h. Expression levels of early odontogenic markers such as *RUNX2* (A), *OSX* (B), *ALP* (C), *OCN* (D) and *DMP1* (E) increased progressively from 0–24 h. Specificity of Wnt5a/ β -catenin signaling was confirmed by gene expression analysis in the presence of Wnt signaling pathway specific inhibitors Box5 and iCRT14. Data are means \pm of triplicates. Means and SDs of fold changes to 0 h are shown. Significant difference * $p < 0.05$; ** $p < 0.01$.

(Fig. 6H and I) suggest that DPP can activate downstream signaling events leading to the polarization of the odontoblast-like cells.

DPP attenuated mineralization in DPSC/Wnt5a- KO cells

To study whether Wnt5a is required for DPP mediated odontogenic differentiation, we used CRISPR to generate a DPSC/Wnt5a KO cell line as described in Material and Method. DNA sequence analysis of puromycin resistant DPSCs revealed an insertion in the gDNA with a predicated frame shifted protein product mismatched with Wnt5a from G₁₉₇ and terminated after G₂₃₄ (Supplement Fig. 1A, B and C). In fact, Wnt5a expression was greatly reduced in DPSC/Wnt5a-KO when compared with DPSCs (Supplement Fig. 2A). Note the mutant Wnt5a protein (MW = 26 kDa) was undetectable as observed by the absence of the low molecular weight bands using anti-Wnt5a antibody, that was raised against a synthetic peptide adjacent to residues Glu₂₀₁ in the Wnt5a protein sequence which would not react with WNT5A mutant containing 1-196 WT WNT5A residues. It is also possible that the mutant Wnt5a protein was not efficiently translated or degraded. DPSC/WNT5A KO cells showed slower proliferation compared to DPSCs with or without DPP treatment (Supplement Fig. 2B). These cells were used in the below-mentioned-studies.

To evaluate the odontogenic differentiation potential of DPSC and DPSC/Wnt5a KO cells were incubated under differentiation conditions with or without DPP for 3 W. The cells were harvested and the expression of key odontogenic markers were assayed via Real-time PCR. Notably, the expressions of pro-odontogenic transcription factors *RUNX2* & *OSX* (Fig. 7A & B) were increased during the differentiation process, stimulation

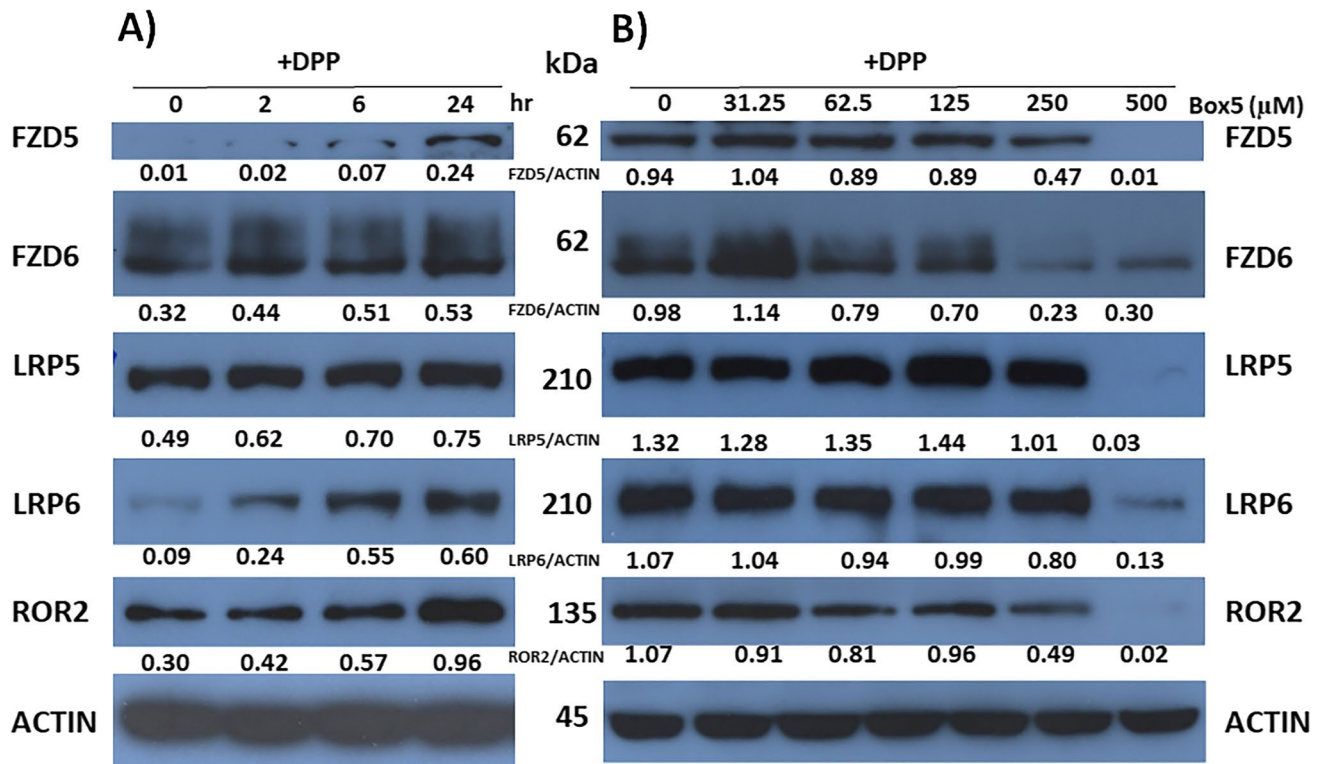


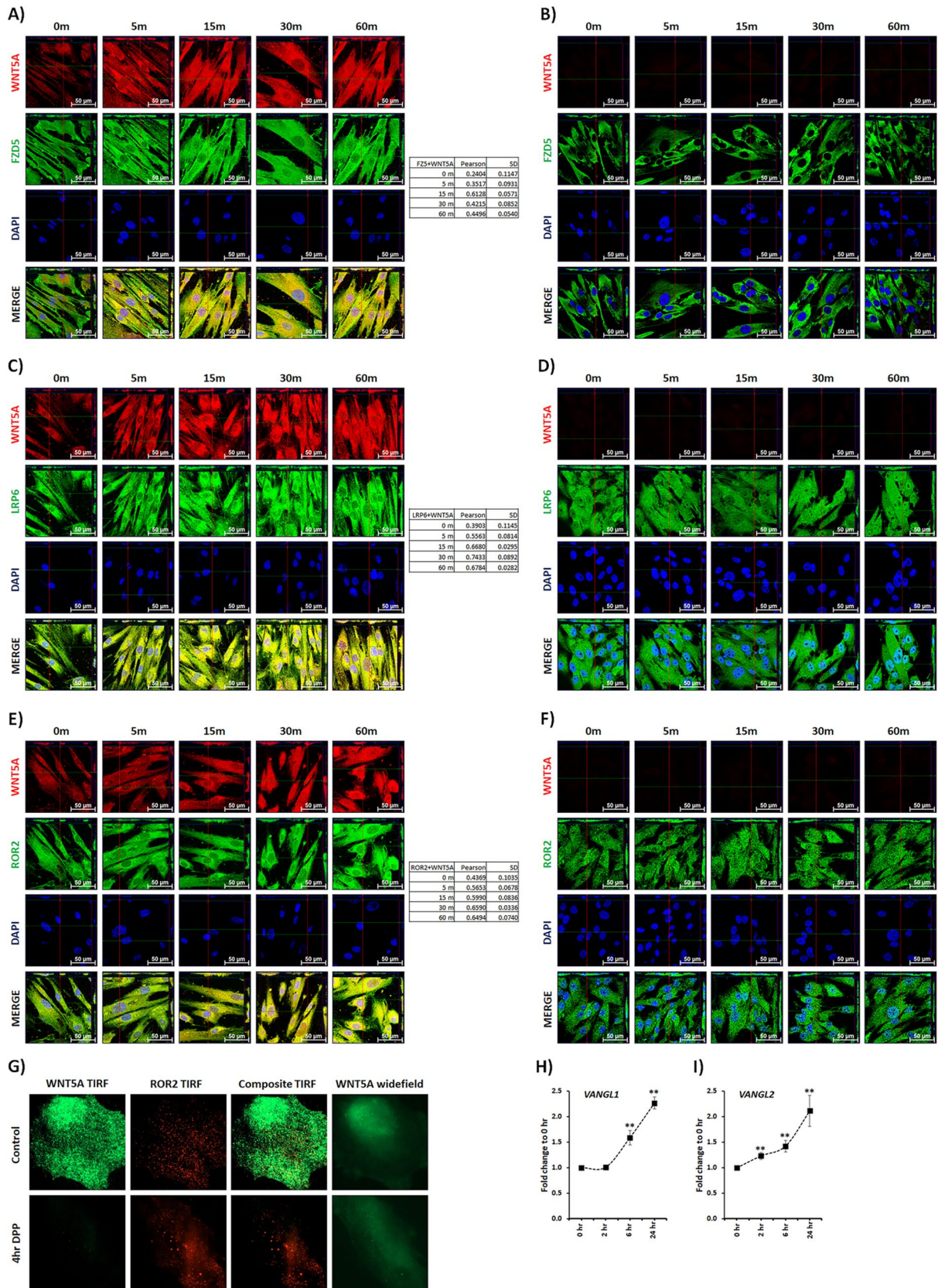
Figure 5. DPP stimulation activates receptors and co-receptors of Wnt5a signaling pathway. **A.** DPSCs were treated with DPP (500ng/ml) for 0, 2, 6, 24 h. Cells were lysed with RIPA buffer and total cell lysates were isolated. Western blotting was performed to detect Wnt5a/ β -catenin receptors FZD5, FZD6, ROR2 and co-receptors LRP5 & LRP6. **B.** DPSCs were treated with varying concentrations of inhibitor Box5 for one hour and stimulated with DPP for 24 h. Western Blotting was performed as above. The density ratios with respect to actin were calculated and indicated on the panel.

with DPP further enhanced their expression levels. However, in Wnt5a KO cells their expression levels were reduced when compared to DPSCs, and addition of DPP showed slightly higher gene expression levels at certain time points (Fig. 7A & B). The expression of *ALP*, a phosphatase involving in phosphate homeostasis increased with DPP in DPSCs and were lower in DPSC/Wnt5a KO cells (Fig. 7C). The expressions of three major ECM genes *COL1A1*, *DMPI*, and *FNI* (Fig. 7D-F), as well as other key matrix genes *OCN*, *OPG*, *OPN*, and *VEGFA* showed similar trends (Fig. 7G-J).

To demonstrate functionality of the differentiated odontoblast-like cells, DPSCs stimulated with DPP were harvested at 0, 1, 2, and 3 W, fixed, and stained with Alizarin Red to detect calcium nodules in the ECM. DPSC, stimulated with DPP exhibited large nodule formation, while DPSC/WNT5A KO cells deposited smaller size nodules regardless of DPP stimulation (Fig. 8A). Quantification of Alizarin Red staining showed higher amounts of Ca^{2+} in DPSCs treated with DPP, while lower values were obtained for DPSC/WNT5A KO cells (Fig. 8B). Similar results were observed when the cell secreted matrix was examined by scanning electron microscopy. Higher amounts of mineralized matrix was seen deposited by DPSCs stimulated with DPP, while smaller mineral deposits were observed in the matrix of DPSC/Wnt5a KO cells (Supplement Fig. 3).

Impaired Wnt5a signaling pathway in DSPP null TG mouse

To demonstrate the in vivo presence of WNT5a, specific receptors and the transcription factor β -catenin in WT and DSPP (precursor of DPP protein) null TG mice, immunohistochemical analysis was performed on postnatal day 3 head sections. DSPP null mice have a phenotype which exhibits low amounts of mineralized dentin with larger unmineralized, predominantly proteinaceous matrix^{11,13}. The pulp chamber contains lower amount of stem cells when compared to the wild type. Analysis of the localization pattern show distinctly lower levels of β -catenin in the pulp region of DSPP null mice within the first molar compared to that of WT mice. Wnt5a was localized around the cell membrane in the WT and intracellular in the KO mice (Fig. 9A & B). In addition, Wnt5a receptors such as Fzd5, Fzd6, Lrp6 and Ror2 were less abundant in DSPP null mouse and showed punctate staining within cells, while in the WT they were predominantly localized on the cell membrane (Fig. 9C-G). Collectively, the localization pattern of Wnt5a and its signaling components confirm impaired Wnt signaling in the absence of DPP.



Discussion

Odontoblasts, the principal dentin forming cells are post-mitotic neural crest-derived cells and are metabolically active throughout the life of the tooth³³. They synthesize the components of the organic matrix of dentin which subsequently calcifies. In addition, they synthesize matrix metalloproteases which can degrade the organic matrix and are capable of transporting calcium ions to the mineralization front. Dentin is a unique, avascular

◀ **Figure 6.** Spatial and temporal analysis of Wnt5a and its receptors and co-receptors with DPP stimulation using immunofluorescence. **A.** Visualization of the expression and interaction between Wnt5a (Red, Alexa Fluor 594) and receptor FZD5 (green, Alexa Fluor 488) in DPSCs. Prominent fluorescent spots at 5–30 min indicate Wnt5a-FZD5 interaction in the merged images. Nuclei stained with DAPI. Scale bar: 20 μ m. **B.** Visualization of the expression of Wnt5a (Red, Alexa Fluor 594) and receptor FZD5 (green, Alexa Fluor 488) in Wnt5a silenced DPSCs. Note DPP stimulation failed to restore Wnt5a expression and its interaction with FZD5. Scale bar: 20 μ m. **C.** Visualization of the expression and interaction between Wnt5a (Red, Alexa Fluor 594) and co-receptor LRP6 (green, Alexa Fluor 488) in DPSCs. Prominent fluorescent spots at 15–60 min indicate Wnt5a-LRP6 interaction in the merged images. Nuclei stained with DAPI, Scale bar: 20 μ m. **D.** Visualization of the expression of Wnt5a (Red, Alexa Fluor 594) and receptor LRP6 (green, Alexa Fluor 488) in Wnt5a silenced DPSCs. Note DPP stimulation failed to restore Wnt5a expression and its interaction with LRP6. Scale bar: 20 μ m. **E.** Visualization of the expression and interaction between Wnt5a (Red, Alexa Fluor 594) and receptor ROR2 (green, Alexa Fluor 488) in DPSCs. Prominent fluorescent spots at 15–60 min indicate Wnt5a-ROR2 interaction in the merged images. Nuclei stained with DAPI. Scale bar: 20 μ m. **F.** Visualization of the expression of Wnt5a (Red, Alexa Fluor 594) and receptor FZD5 (green, Alexa Fluor 488) in Wnt5a silenced DPSCs. Note DPP stimulation failed to restore Wnt5a expression and its interaction with ROR2. Scale bar: 20 μ m. **G** Representative TIRF microscopy image showing the presence of Wnt5a (green) & Ror2 (red) on the plasma membrane and their reduced levels with DPP stimulation. Total RNA was isolated from DPSCs stimulated with DPP and quantitative RT-PCR analysis performed. Fold changes were obtained relative to 0 h. Expression levels of Vangl1 (**H**) increased from 0–6 h and Vangl 2 (**I**) progressively from 0–24 h. Means and SDs of fold changes to 0 h are shown. Significant difference $**p < 0.01$.

mineralized connective tissue that forms the bulk of the tooth¹. It encloses a richly innervated and highly vascularized soft connective tissue the dental pulp.

The major phosphoprotein in the dentin matrix is an aspartic acid and serine-rich protein called dentin phosphophoryn (DPP). DPP appears to be synthesized as a part of a larger compound protein, dentin sialophosphoprotein (DSPP)⁹. DPP is a highly acidic protein that binds Ca^{2+} avidly and is thus linked to matrix mineralization^{34,35}. Besides its function in matrix mineralization, we and others have shown that DPP functions as a signaling molecule. We have demonstrated that progenitor stem cells treated with DPP stimulates the release of intracellular calcium¹⁵. This depletion of calcium from the endoplasmic reticulum evokes a number of downstream responses. We hypothesize that this event is responsible for the activation of downstream Wnt5a/ β -catenin signaling events.

Wnt signaling is evolutionarily conserved group of signaling pathways that regulate a diversity of processes ranging from embryonic development to adult tissue homeostasis. Depending on the cell/tissue type, Wnt5a binds to a number of distinct trans-membrane receptors resulting in the activation of diverse signaling events resulting in specific cell behaviors. Wnt5a falls into the family of non-canonical Wnt ligands and activates several downstream signaling events including the activation of the Wnt master regulator, β -catenin. Wnt5a is essential for proper skeletal development as homozygous Wnt5a knockout mice exhibit perinatal lethality, due to developmental defects^{36,37}. Further, appendicular structures fail to extend from the primary body axis³⁷. The defect in morphogenesis is associated with decreased cell proliferation in tissues crucial to outgrowing structures. During odontogenesis, very little is known about the role of Wnt5a. However, published report show that Wnt5a deficient mice exhibit retarded tooth development as early as E16.5 resulting in smaller and abnormally patterned teeth with a delay in odontoblast differentiation^{18,24}. These defects are associated with reduced proliferation in the dental epithelium and the mesenchyme. Among the Wnt ligands, only Wnt5a was intensely expressed in the dental epithelium and the mesenchyme during embryonic days 14–17. Cleft palate phenotype was observed in Wnt5a null-mice, and the phenotype was attributed to defective cell migration^{38,39}. Interestingly, during tooth development, both Wnt5a and DSPP transcripts have been reported to be expressed in differentiating odontoblasts at the late bell stage^{40–42}.

Understanding the molecular mechanism that mediates the differentiation of adult stem-cells to regenerate the dentin-pulp complex is of great importance in regenerative dental medicine. This process requires a fine balance between cell proliferation and differentiation. Differentiation of DPSCs to fully functional odontoblasts require selective activation of specific programs of gene expression. In vivo, these cells are believed to spontaneously differentiate when placed in the correct microenvironment where both intracellular and extracellular signals regulate the differentiation process.

In this study, we show that both DPP and Wnt5a are localized in the extracellular matrix of DPSCs. This is not surprising as Wnt ligands, including Wnt5a exert their signaling functions from the ECM by binding to specific cell-surface receptors. We further showed that extracellular vesicles such as exosomes isolated from DPSCs contain both Wnt5a and DPP as components of their cargo. Wnts are lipid modified and therefore hydrophobic, hence it is reasonable that Wnt5a is secreted in exosomes^{43,44}. We had previously shown that DPP is highly acidic and that intracellular DPP was transported to the ECM in exosomes⁹. Ultrastructural analysis using immunotEM, confirmed that both DPP and Wnt5a are constituents of the exosomal cargo of DPSCs. An interesting study showed that Wnt5a signaling induces a Ca^{2+} -dependent release of exosomes⁴⁵ from malignant melanoma cells. Therefore, it is possible that DPP-mediated Wnt5a activation has a broader function by inducing exosome release containing cargo that aids differentiation and matrix mineralization.

Interestingly, we found that DPP induced the expression of Wnt5a in DPSCs which promoted their differentiation into odontogenic lineage. Wnt5a signaling has been implicated in regulating multiple cellular processes. We had previously demonstrated that NF- κ B is functionally activated by DPP in DPSCs²⁹. In this

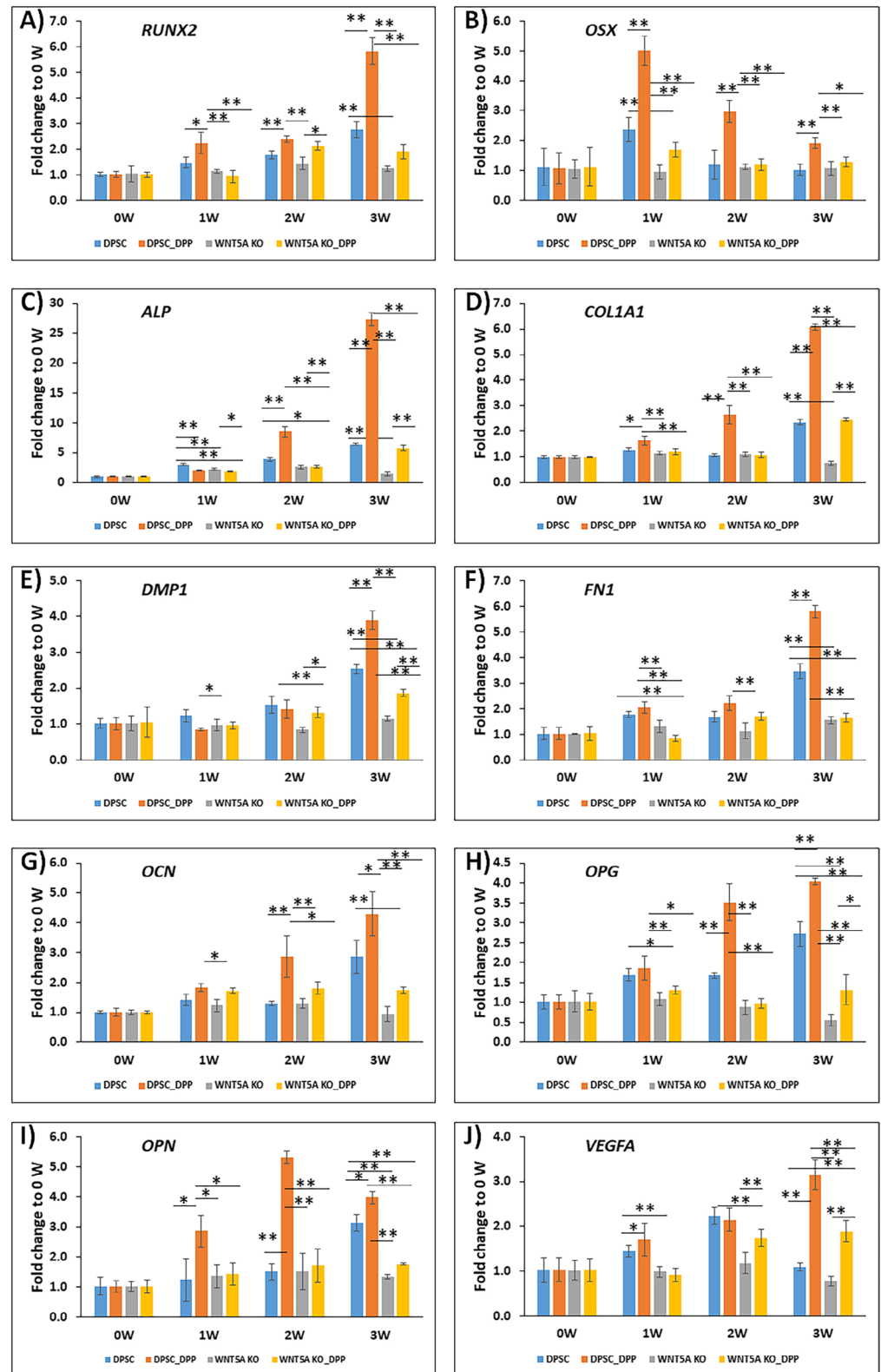


Figure 7. Effect of DPP-mediated Wnt/ β catenin signaling on the terminal differentiation of DPSCs into odontoblastic lineage. DPSCs and DPSC/Wnt5a-KO cells were stimulated with or without DPP and cultured under differentiation conditions for 0–3 weeks. Total RNA was isolated at the indicated time points and quantitative RT-PCR analysis performed. Fold changes were obtained relative to day 0. Expression levels of odontogenic markers such as (A) *RUNX2*; (B) *OSX*; (C) *ALP*; (D) *COL1A1*, (E) *DMP1*, (F) *FN1*; (G) *OCN*; (H) *OPG*; (I) *OPN*; (J) *VEGFA*. Gene expression fold changes calculated at the relative ratios to day 0 and means and SDs of changes and comparisons are shown. Note lower gene expression levels in Wnt5a silenced DPSCs even with DPP stimulation. * $p < 0.05$; ** $p < 0.01$.

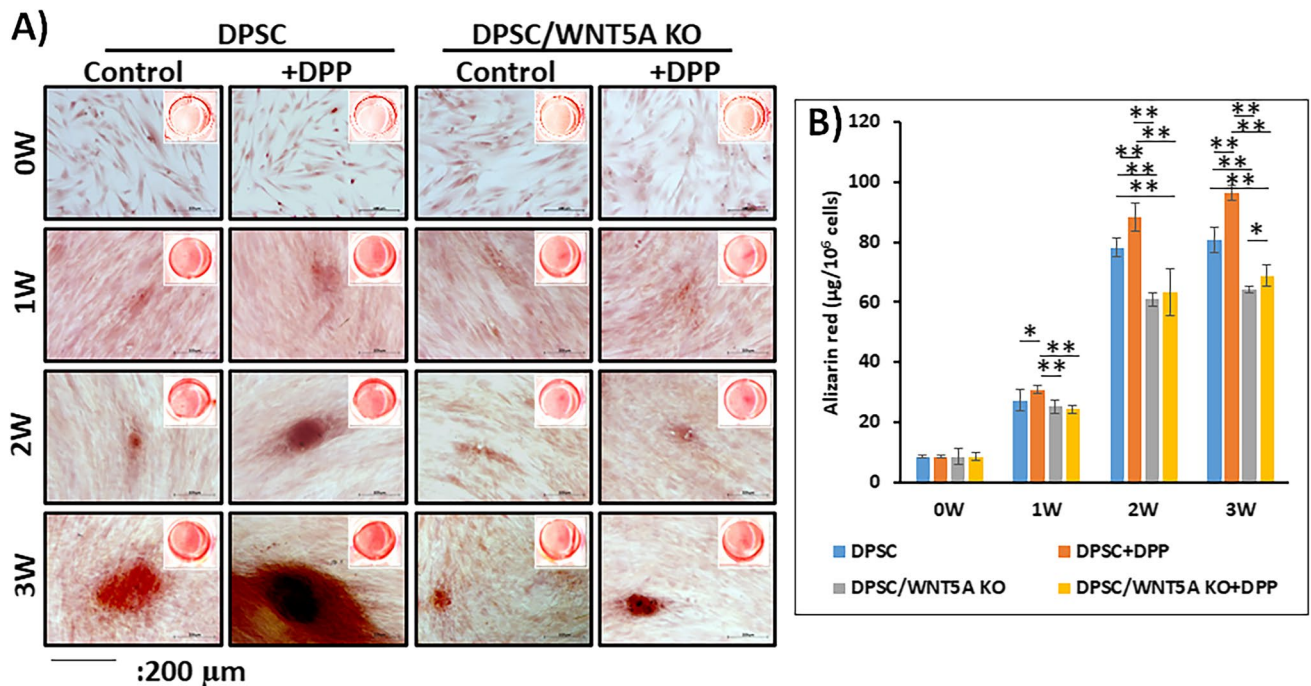


Figure 8. Silencing Wnt5a in DPSCs impair their ability to assemble a calcified extracellular matrix. **A.** DPSCs and DPSC/Wnt5a-KO cells were stimulated with or without 500ng DPP and cultured under differentiation conditions for 0–3 weeks. The mineralized nodules containing calcium were visualized using Alizarin Red staining. Note the small size of the mineralized nodule in the Wnt5a-silenced DPSCs. Insets were scanned images of a well from 12 well tissue culture plate. **B.** Quantitative measurement of the calcium content in the deposited nodule was determined by measuring the absorbance of the eluted Alizarin Red stain at 562 nm on a multiplate reader using a standard calcium curve. Statistically significant differences are indicated at 1, 2 and 3 weeks. *p, 0.05, **p, 0.01.

study, we demonstrate for the first time that DPP activates Wnt5a in DPSCs. Treatment of DPSCs with NF- κ B inhibitors, TPCA-1 & JSH-23, abrogated Wnt5a mRNA and protein expression with DPP stimulation, indicating the requirement of NF- κ B in promoting Wnt5a expression. Further, Wnt5a promoter containing the NFKB binding site, also showed reduced activity with TPCA-1 treatment and DPP stimulation. ChIP analysis confirmed the binding of p65 to specific NF- κ B binding site on the Wnt5a promoter. Having demonstrated the role of NF- κ B on regulating odontogenic markers with DPP stimulation, therefore, we examined the involvement of Wnt5a signaling in the odontogenic differentiation process.

To demonstrate that DPP-mediated Wnt5a activation promoted odontogenic differentiation, we inhibited the Wnt5a/ β -catenin signaling pathway at two different levels i.e., in both the cytoplasm and in the nucleus in DPSCs. The Wnt5a-derived hexapeptide Box5, acts as a Wnt5a antagonist in the cytoplasm and inhibits Ca^{2+} signaling and ICRT14 a drug that acts in the nucleus inhibiting direct interactions between β -catenin and TCF4, thereby blocking the transcriptional function of β -catenin. Interestingly, both treatment modes attenuated the expression of odontogenic differentiation markers such as Runx2, osterix, alkaline phosphatase and osteocalcin. The differentiation process was also monitored until 3 weeks in Wnt5a-silenced DPSCs. At all-time points, the transcripts for the differentiation markers were downregulated in the Wnt5a-KO cells with and without DPP stimulation. These findings indicate an important signaling function of DPP that promotes the odontogenic differentiation of DPSCs by activating the expression of Wnt5a.

Strikingly, in this study ICRT14 the Wnt/ β catenin drug was able to inhibit the odontogenic differentiation of DPSCs suggesting that Wnt5a mediates differentiation through the transcription factor β -catenin. Confocal imaging shows the nuclear translocation of β catenin with DPP stimulation, and this effect was abrogated in the presence of TPCA-1 and in Wnt5a-KO DPSCs. Increase in nuclear β catenin accumulation was also observed with DPP stimulation. Wnt5a does not typically activate β catenin, however, published reports show that Wnt5a is capable of both inducing and repressing β catenin signaling in vivo depending on the time and site of expression and the receptors expressed by receiving cells⁴⁶. In vivo study show that loss of β -catenin leads to the arrest of odontogenesis during early tooth development⁴⁷. The conditional ablation of β -catenin in osteoblast and odontoblast causes the malformation of the root dentin and cementum⁴⁸. Amerongen et al. have shown that Wnt5a causes activation of Wnt/ β -catenin signaling in the developing skull⁴⁶. One of the downstream signaling pathways of Wnt5a is mediated through the translocation of β -catenin to the nucleus where binding to DNA and transcriptional regulation occurs. This implies that the odontogenic differentiation of DPSCs, mediated by DPP-activated Wnt5a is driven by β -catenin/TCF signaling.

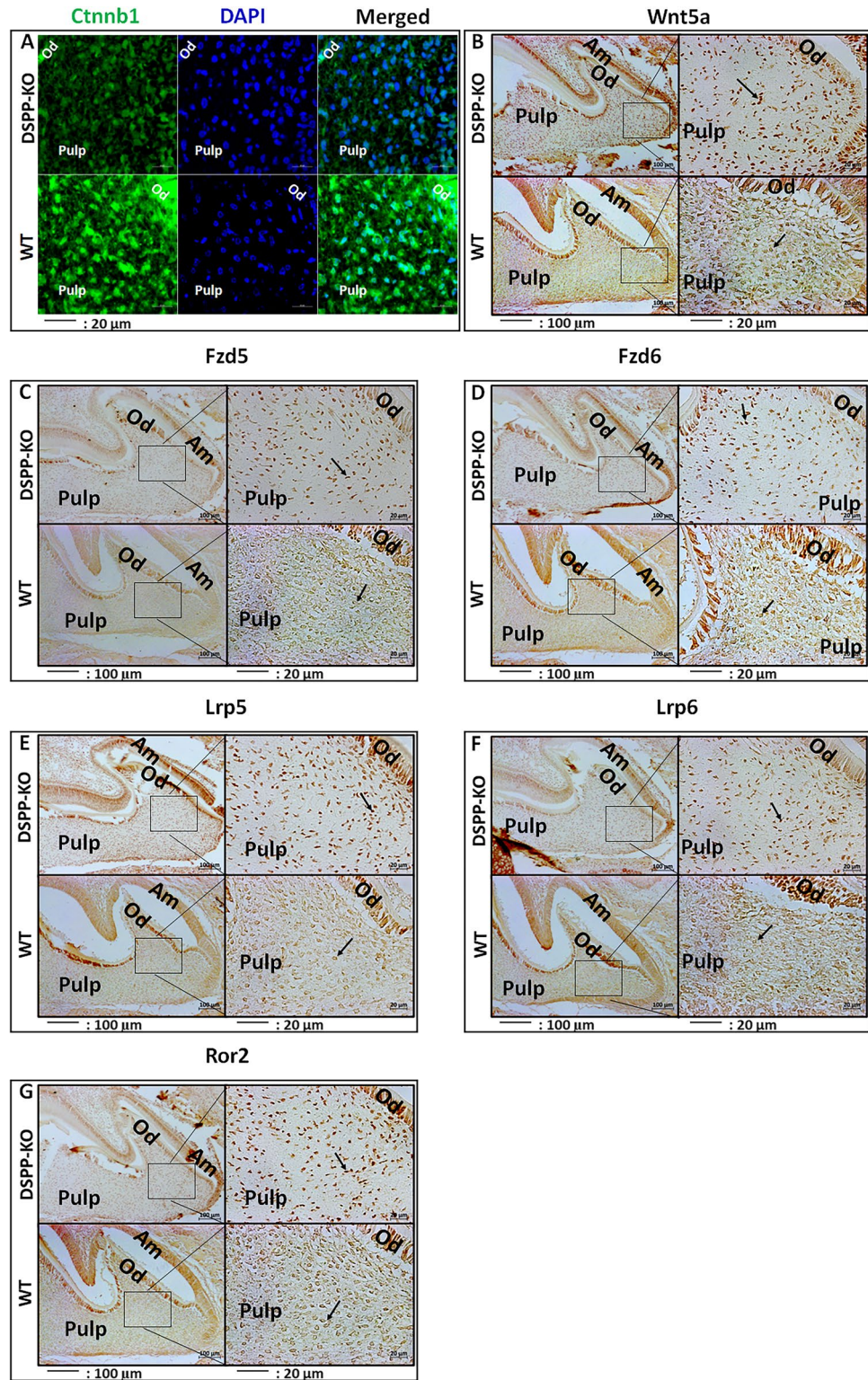


Figure 9. Expression of Wnt5a and signaling components of Wnt5a in WT & DSPP-KO mice. Post-natal day 3 DSPP null mice and their matched wild type mice heads were used for immunohistochemical analysis. Sections were treated with primary antibodies against β -catenin (A); Wnt5a (B); Fzd 5(C); Fzd6(D); Lrp5 (E); Lrp6 (F) and Ror2 (G). Boxes marked are higher images showing staining in the dental pulp cells.

Wnt5a can induce multiple signaling pathways which are highly dependent on the available receptors. Signals are initiated at the plasma membrane when a Wnt ligand binds to its cognate Frizzled receptor as well as to the Wnt co-receptor, low density lipoprotein-related protein 5 (LRP5). This activates the cytoplasmic protein Disheveled (Dvl) and Dvl inhibits phosphorylation of β -catenin by GSK-3 β , thus causing β -catenin stabilization and accumulation in the cytoplasm, before translocation to the nucleus, where it binds with members of the T-cell factor (TCF) and lymphoid enhancer factor (LEF) transcription factors, resulting in the enhanced expression of target genes⁴⁹. To date there are 10 identified Fzd receptors in mammals and the specificity of the signal depends on the affinities between the Fzd family members and 19 different Wnt ligands. In this study, DPP-mediated Wnt5a activation in DPSCs upregulated the expression of Fzd5/Fzd6 as treatment of Wnt5a inhibitor Box5 downregulated their expression. Confocal imaging further demonstrates puncta formation and internalization of Wnt5a and Fzd5. Silencing of Wnt5a abrogated these effects. However, silencing of Wnt5a in DPSCs affected the localization of Fzd5 on the cell membrane. Thus, Fzd5, would be the key receptor that initiates the signaling process by binding to Wnt5a at the cell surface. Similarly, coreceptors LRP5 and 6 were downregulated when DPSCs were treated with Box5 and stimulated with DPP, however, LRP5 expression was completely abrogated by silencing Wnt5a. Several published observations suggest that LRP5 regulates osteoblastic proliferation and differentiation and reduced LRP5 expression appears to negatively regulate bone mass⁵⁰. In this study, our findings indicate that in DPSCs, expression of Lrp5 is increased with DPP stimulation and can transduce the Wnt-Fzd5 signaling pathway to activate β -catenin. Wnt5a has been reported not to interact with LRP6 but interact with Lrp5 and Frizzled 4 to initiate the β -catenin signaling pathway^{31,51}.

Wnt5a specific receptor Ror2 (Receptor tyrosine kinase -like orphan receptor 2) is one of the non-canonical Wnt receptors. Several studies show the pivotal role that Ror2 binds Wnt5a and functions in cell polarity, proliferation, differentiation, migration and aging. Interestingly, in the presence of Wnt5a, Ror2 can inhibit or activate canonical Wnt signaling at the level of TCF/LEF-mediated gene transcription⁵². During tooth development in mice, *Ror2* is expressed in the dental epithelium and mesenchyme at embryonic stages^{18,53–55}. In humans, *Ror2* mutations cause defects in several bone types and patients with recessive Robinow syndrome exhibit defects in tooth formation and eruption demonstrating the importance of Ror2 in cellular differentiation^{55,56}. In a recent publication, Ma et al. showed that loss of *Ror2* in the dental mesenchyme leads to delayed root elongation, leading to shortened roots in a conditional knockout mouse model⁵⁵. Specifically, mesenchymal Ror2 was shown to regulate cell proliferation, odontoblast differentiation in the apical region of the tooth during root formation by regulating Cdc42 a potential downstream modulator of Ror2 signaling⁵⁷. Using TIRF microscopy, we have shown that DPP stimulation can modulate the binding of Ror2 with Wnt5a and promote the internalization of Wnt5a- Ror2 complex from the plasma membrane resulting in activation of the Ror2 signaling cascade. Wnt5a-Ror2 signaling have been shown to potentiate osteogenic differentiation of hMSC in a Ror-2 dependent manner and enhanced bone formation in the mouse explant cultures⁵⁸. In this study, immunohistochemical analysis, show the spatial and temporal expression of Ror2 in the dental pulp cells and in the odontoblasts while mice deficient in DPP had lower expression and the mice exhibited impaired odontoblast differentiation. The presence of other cell polarity genes such as Van Gogh (Vangl1 & 2) might regulate polarization of the odontoblasts during the differentiation process. It has been shown that *Wnt5a* has the strongest effects in inducing Vangl2 phosphorylation. Wnt ligand receptors in DPSCs suggest that it is possible that Ror2 might oligomerize with other surface proteins such as Frizzled receptors and form a complex with LRP5/6 in response to DPP-mediated Wnt5a activation. Through such a mechanism, Wnt5a could enhance the expression of downstream β -catenin target genes. The ability of DPSCs to generate an appropriate receptor context may depend on DPP-mediated signaling events.

Differentiation of dental pulp stem cells to functional odontoblasts would be highly beneficial to regenerate dentin. However, odontoblast differentiation is a complex process regulated by several signaling pathways including Wnts. Using Wnt5a-silenced cells we demonstrated that DPP mediated Wnt5a activation was responsible for the regulation of several odontogenic differentiation transcripts such as DMP1, FN (fibronectin) OCN, OPG, OPN and VEGFA. In the presence of DPP, an increase in the expression of the differentiation markers were observed from 1 to 3 weeks in differentiation media. Interestingly, in the absence of Wnt5a, expression levels were downregulated indicating the inactivation of odontoblast differentiation. Terminal differentiation of odontoblasts was confirmed by the functional Alizarin Red assay. Corresponding to the gene expression pattern, matrix mineralization increased from 1 to 3 weeks as shown by the increased calcium deposition in DPSCs stimulated with DPP. However, in Wnt5a silenced DPSCs there was a reduction in mineralization as shown by the weak Alizarin Red staining and DPP stimulation did not rescue the formation of mineralized ECM. These observations identify a previously unrecognized role of DPP in mineralized matrix formation by activating the Wnt5a/ β -catenin signaling to promote the differentiation of DPSCs.

Temporal and spatial analysis confirm the presence of the various components of the Wnt5a/ β -catenin signaling pathway. Immunohistochemical analysis confirm the presence of Wnt5a and β -catenin in the dental pulp cells and in the differentiating odontoblasts of developing tooth molars and mice with loss of DPP, abrogates the expression level of Wnt5a and impairs the nuclear translocation of β -catenin. Furthermore, expression levels of Wnt5a receptor Ror2 and co-receptors LRP5/6 were abrogated in the odontoblasts and dental pulp cells in DPP-silenced mice. Thus, differentiation of dental mesenchymal cells to functional odontoblasts requires DPP-mediated activation of Wnt5a-stimulated β -catenin dependent transcription.

Conclusion

Adult stem cells found in the dental pulp are an important source of cells for dentin repair and regeneration. During the odontogenic differentiation of DPSCs, several signaling events are activated. The data presented above strongly suggest that DPP in the matrix can activate Wnt5a-mediated signaling events and promote their differentiation into odontoblasts. The paradox with DPP-mediated Wnt signaling is the activation of Wnt5a

which promotes the expression of Wnt-target genes in a β -catenin dependent manner. Among the various receptors that interacted with Wnt5a are FZD5 and coreceptor LRP6. Furthermore, Wnt5a can bind to Ror2 to promote polarization of DPSCs during the odontoblast differentiation process. Regeneration of functional odontoblasts by DPP-mediated Wnt activation has therapeutic implications, as strategies to deliver Wnts is not a trivial task. The hydrophobic nature of Wnt proteins makes isolation and tissue delivery very challenging. Therefore, DPP-mediated Wnt5a signaling may be a therapeutic target for the repair and regeneration of impaired dentin mineralization.

Materials and methods

Cell culture

Dental pulp stem cells (DPSCs, a kind gift from Dr. Shi, University of Pennsylvania) were cultured in growth media (α -minimum Eagle's medium, Thermo Fisher Scientific) supplemented with 10% fetal bovine serum (FBS; Thermo Fisher Scientific) and 1% Antibiotic-Antimycotic (100X) (Thermo Fisher Scientific) in a humidified CO₂ incubator at 37 °C. At ~80% confluency, cells were split at 1:3 ratio (one passage), and cells from passage 6 to 12 were used in all experiments⁵⁹.

Isolation of total cellular proteins and immunoblotting

Recombinant DPP protein was expressed and purified as described previously¹⁴. For cell culture, DPSC cells were seeded at 70% confluency in growth media. After allowing the cells to attach for 6 h, the cells were cultured with the media containing 1% FBS overnight. The cells were then treated with or without the small molecule inhibitor TPCA-1²⁹ (NF- κ B pathway inhibitor) for 1 h and then stimulated with DPP (500 ng/ml) and further experiment was conducted as previous publication²⁹. Briefly, at the indicated time points, cells were harvested and lysed with RIPA buffer (Cell signaling) containing a cocktail of protease and phosphatase inhibitors (Millipore). The lysate was subjected to centrifugation at 14,200 rpm for 15 min at 4 °C and the supernatant collected and used as total cellular proteins. The protein concentration was measured using Bio-Rad Protein Assay Dye Reagent (BIO-RAD,) with BSA being the standard. 30 μ g of total proteins were separated by electrophoresis on a 10% SDS-PAGE gel and transferred onto a polyvinylidene fluoride (PVDF) membrane (BIO-RAD). The membranes were incubated with the following primary antibodies overnight at 4 °C: anti-Wnt5A/B rabbit polyclonal antibody (2530, Cell Signaling), anti-LRP5 (Rabbit mAb #5731), anti-LRP6 (Rabbit mAb #3395), anti-Frizzled 5 (Rabbit 06-756) from Sigma/Millipore, anti-Frizzled 6 (Rabbit mAb #5158), ROR2 (Rabbit mAb #88639). They were washed with PBS, incubated with HRP conjugated anti-rabbit or anti-mouse secondary antibodies (7076, Cell signaling), β -actin mouse monoclonal antibody (3700, Cell signaling). The bands were visualized using SuperSignal™ West Pico chemiluminescent Substrate (Thermo Scientific) with X-ray film according to the manufacturer's protocol. The membrane was then stripped with Restore PLUS Western Blot Stripping Buffer (Thermo-Scientific) and probed with anti- β -actin mouse monoclonal antibody or (Tubulin T3168 Sigma) as internal control. The images were scanned and band densities were measured using ImageJ (1.52c). To monitor expression of Wnt receptors, the Wnt5a ligand was blocked by pretreating cells with Box5⁶⁰ (a Wnt5A antagonist, N-butyloxycarbonyl hexapeptide M₃₃₂DGCEL₃₃₇ of NP_003383.4) at indicated concentrations for 1 h. The cells were then stimulated with DPP for 24 h and processed as above.

Subcellular fractionation

DPSC cells were seeded and stimulated with DPP as described above and harvested at 0, 0.5, 6 and 24 h. The cytoplasmic and nuclear fractions were obtained with the NE-PER nuclear and cytoplasmic extraction reagents according to the manufacturer's protocol (Thermo Scientific). Sodium dodecyl sulphate (SDS) loading buffer was added and subjected to Western blot analysis. Actin was used as protein loading control while tubulin and lamin A/C (#4777 Cell signaling) were used for cytoplasmic and nuclear fractions respectively.

Isolation of the ECM

DPSCs overexpressing DPP were grown to confluence on cover glass for ECM isolation according to published protocol⁶¹. Cells were lysed by incubating for 15 min with 0.5% TritonX-100, 0.01 M sodium phosphate, 0.15 M NaCl, pH 7.4 at 37 °C and 5%CO₂ followed incubation for 10 min under the same conditions with 0.25 M ammonium hydroxide. The coverglass were then washed with 0.02 M Tris-HCl, pH 7.4, 0.15 M NaCl and 0.05% Tween-20. A final wash was performed with HBS buffer. The ECM was then fixed with 4% formaldehyde and subjected to immunostaining with rabbit anti Wnt5a antibody (1/100), rabbit anti -DPP antibody (1/2000).

Quantitative real time PCR (qRT-PCR)

DPSC cells were treated as described above and harvested at indicated times points. Before addition of DPP, DPSC cells were pretreated with iCRT14 and Box5 for 1 h. Total RNA were obtained from cells using TRIzol Reagent (Invitrogen). cDNAs were synthesized and real-time PCR was conducted as described previously²⁹. The gene expression levels were estimated by the 2^{- $\Delta\Delta$ CT} method with GAPDH gene expression level as a internal control. Primers were synthesized by IDT (Integrated DNA Technologies, Inc). The primer sequences are listed in Table 1.

ELISA to quantitate Wnt5a secretion

DPSCs were seeded in growth media and then cultured with 1% FBS overnight. The cells were then treated with or without TPCA-1 for 1 h and then stimulated with DPP 9500ng/ml). At indicated time points the conditioned media were collected and stored at -80 °C. Direct ELISA was performed by mixing the conditioned media with 50mM carbonate buffer pH 9.4 and coated onto a 96-well Costar Assay plate (Corning) for 24 h at 4 °C. After blocking with 5% BSA in PBS, the samples were incubated for 2h with anti-wnt5a antibody, followed by

Gene Name	Accession	Sequence
ALP	NM_001127501	AAC ATC AGG GAC ATT GAC GTG
		GTA TCT CGG TTT GAA GCT CTT CC
OSX	AF477981	GCC AGA AGC TGT GAA ACC TC
		GCT GCA AGC TCT CCA TAA CC
RUNX2	NM_001015051	TGG TTA CTG TCA TGG CGG GTA
		TCT CAG ATC GTT GAA CCT TGC TA
FN1	NM_212482.2	CAG TGG GAG ACC TCG AGA AG
		GTC CCT CGG AAC ATC AGA AA
COL1A1	NM_000088	GAG GGC CAA GAC GAA GAC ATC
		CAG ATC ACG TCA TCG CAC AAC
OPN	NM_000582	AGG AGG AGG CAG AGC ACA G
		GAG ATG GGT CAG GGT TTA GC
OPG	NM_002546	CAA AGT AAA CGC AGA GAG TGT AGA
		GAAGGTGAGGTTAGCATGTCC
OCN	NM_199173	CAC TCC TCG CCC TAT TGG C
		CCC TCC TGA TTG GAC ACA AAG
DMP1	NM_004407.3	AAT TCT TTG TGA ACT ACG GAG GG
		CAC TGC TCT CCA AGG GTG G
VEGFA	NM_001171627	AGG GCA GAA TCA TCA CGA AGT
		AGG GTC TCG ATT GGA TGG CA
WNT5A	XM_011534088	GCC AGT ATC AAT TCC GAC ATC G
		TCA CCG CGT ATG TGA AGG C
GAPDH	NM_001357943	GGA GCG AGA TCC CTC CAA AAT
		GGC TGT TGT CAT ACT TCT CAT GG

Table 1. DNA oligoes for quantitative PCR.

incubation with anti-rabbit IgG HRP for 2 h. After wash, the samples were developed using 1-Step Ultra TMB-ELISA Substrate Solution (Thermo- Scientific) according to manufacturer's protocol. Absorbance at 450 nm was measured with a plate reader. Recombinant Wnt5a (CUSABIO, USA) was used to generate a standard curve.

Transient transfection and promoter analysis by luciferase assay

The experiments were carried out as in previous publication²⁹. One day prior to transfection, 3×10^5 cells were seeded in one well of a 12-well tissue-culture plate (BD Biosciences, San Jose, CA). After 12 h, co-transfections were conducted using the transfection vector mixture (total 333 ng) containing NF-kb RE luc reporter construct (300 ng, a kind gift from Dr. Lyndon F Cooper of University of Illinois Chicago) or p420, a WNT5A promoter luc reporter construct (300ng, a kind gift from Dr. Karen Katula of University of North Carolina Greensboro). CMV/Renilla luciferase vector (33 ng, Promega) was used as transfection efficiency control. 0.6 μ l of transfection agent Lipofectamine 2000 (Invitrogen) was added to the mixture, and co-transfections were conducted according to the manufacturer's instruction. Sixteen hours later, the cells were cultured in α -minimum Eagle's medium containing 1% FBS with or without TPCA-1 (10 μ M) for 30 min followed by DPP (500ng/ml) stimulation. After 48 h, cell lysates were prepared using passive lysis buffer (Promega). Luciferase activities in the lysates were measured using a dual luciferase assay system (Promega) using a plate reader (Synergy 2, BIOTEK).

Chromatin immunoprecipitation (ChIP)

ChIP assays were performed with a commercially available CHIP-IT high sensitivity kit following the manufacturer's protocol (Active Motif North America, Carlsbad, CA) and as previously reported²⁹. Briefly, 1×10^6 DPSC's were treated with DPP (500 ng/ml) for 1–2 h and anti-p65 antibody (ab16502, Abcam) was used in immunoprecipitation, while the normal isotype-matched IgG from the same species served as negative control. RT-PCR was used to amplify DNA fragments using specific primers. Relative amount of the DNA fragments was calculated as percentages to that of the input DNA used in the ChIP assay. The ratio of relative DNA amount of p65 bound to that of IgG were used as enrichments of NF-kB binding.

Immunofluorescence

Similar to previous publication²⁹, DPSCs were seeded on glass coverslips and cultured in growth media until 70–80% confluency. They were then cultured in 1% serum overnight and treated with TPCA-1 or Box5 followed by DPP (500 ng/ml) stimulation at the indicated time points. DPSC/Wnt5a KO cells were used and treated with DPP (500ng/ml) as stated above. In addition, Wnt5a recombinant protein (500ng/ml, R & D Systems) or PF-L6 (1nM, a kind gift from AntlerA Therapeutics) were used as positive controls to treat DPSCs to monitor nuclear accumulation of β -Catenin. PF-L6 was a specific agonist antibody of FZD and LRP6 and have been reported to activate Wnt/Frizzled pathways in cells, organoids and mice⁶². The treated cells were washed once with cold

PBS and then fixed in 10% neutral formalin at 4 °C for 1 h. Fixed cells were permeabilized with 0.25% Triton-X in PBS for 30 min at 37 °C and incubated with β -Catenin antibody (Sigma) overnight at 4 °C, followed by incubation with fluorescent goat-anti mouse Alexa 488 (Abcam) at RT for 1 h. The cover glass was mounted onto a glass slide using mounting agent with DAPI (Vectorlab). Cells were imaged with a Zeiss 710 Meta Confocal Microscope at the UIC RRC Facility. Pearson's colocalization coefficient was obtained using Zen software 3.7.

TIRF microscopy analysis

HEK293T cells transfected with Wnt5a-EGFP and Ror2-mCherry were seeded on 35 mm collagen coated glass bottom dishes (MatTek Corporation, Ashland MA, United States) and cultured under normal growth conditions. The cells were subsequently stimulated with DPP and imaged using a Zeiss Laser TIRF Microscope.

CRISPR-Cas9 based knockout of Wnt5A in DPSCs

Lenti CRISPR vector (LV01/WNT5A) containing predesigned CRISPR gRNAs targeting Wnt5a were purchased from Sigma (<http://www.sigmaaldrich.com>. WNT5A: HSPD0000044593).

Knockout of Wnt5a in DPSCs were performed as recommended by the manufacturer. Briefly, the LV01/WNT5A, together with the psPAX2 (Addgene), pMD2.G (Addgene), and pHPV17 plasmids were transfected in 293FT cells (Invitrogen). After 48 h, virus-containing supernatant was collected, and centrifuged at 1000 g for 10 min to remove cell debris, followed by 75,000 g for 4 h at 4 °C to collect the pellet containing viral particles. The collected viral particles were used to infect DPSC cells. After 72 h, the DPSCs were selected with 1 μ g/ml puromycin for 3 to 5 days. The drug resistant cells were pooled and chromosomal DNA was extracted from DPSC/Wnt5a KO cells with Direct PCR Lysis Reagent (Viagen Biotech, Inc). The DNA region flanking targeted gDNA was PCR amplified using Platinum™ Taq DNA Polymerase (Invitrogen) with primer pair (WNT5A_FW_913: -CCT CGT TGT TGT GCA GGT TC-; WNT5A_RV_1218: -GTG ATC CCT TGT CCT CAC CC-). PCR products were cleaned with QIAquick Gel Extraction Kit (QIAGEN) and analyzed by Sanger sequencing at RRC facility at UIC. Sequences were checked for WNT5A gene mutation. Western blot was also performed to demonstrate knockdown of WNT5A protein. These cells were designated as DPSC/WNT5A KO were used for further experiments.

Cell proliferation

DPSC and DPSC/Wnt5a KO cells were seeded in 96 well plate and cultured for 24 h at 37 °C, 5% CO₂. They were then treated with DPP at 500 ng/ml for the indicated time points. CellTiter 96 Aqueous One Solution Reagent (Promega, Cat. No. G3580) was used to monitor the live/dead cell numbers according to the manufacturer's instructions. The absorbance was recorded on a multi-plate reader at 490 nm (Synergy HT, BIO-TEK INSTRUMENTS, INC., WINOOSKI, VERMONT USA).

In vitro mineralization assay and nodule detection by alizarin red staining and SEM

In vitro mineralization assay and nodule detection by alizarin red staining and SEM were conducted as in previous publication²⁹. DPSC's and DPSC/Wnt5a KO cells were cultured in growth media until 80% confluent. The cells were cultured in odontogenic differentiation media (growth media containing 10 mM β -glycerophosphate (Sigma Aldrich), 0.50 mM ascorbic acid (Sigma-Aldrich), and 10 nM dexamethasone (Sigma-Aldrich)). The cells were then stimulated with or without DPP (500ng/ml) for 0, 7, 14 and 21 days. At each time point, the cells were washed with PBS and fixed in 10% neutral formalin at 4 °C for 4 h. The cells were stained with 2% Alizarin Red S Solution (Sigma) for 30 min, then rinsed with water. The plates were scanned to visualize the overall staining pattern and higher magnification images were obtained with a light microscope (Zeiss Axio Observer D1). Colorimetric method was used to determine the calcium concentration in the cell matrix.

For SEM analysis, the cells were seeded on a cover glass (12 mm, Invitrogen) and cultured under differentiation condition as described above. At indicated time point, the cells were briefly washed with PBS twice, fixed in 10% neutral buffered formalin for 2 h at room temperature. The cells were washed with water, followed by dehydration with gradient ethanol, and treated with hexamethyldisilazane (Electron Microscopy Sciences, Hatfield, PA) and dried. The cover glass with the cells were mounted on an M4 aluminum specimen (Ted Pella, Inc., Redding, CA), coated with 10 nm gold/palladium metal film with a Cressington 208 h sputter coater (Cressington Scientific Instruments UK, Watford, England (UK)). The topography data were obtained with a scanning electron microscope (JEOL JSM-IT500HR, JEOL USA, Inc., Peabody, MA). The following conditions were used to acquire the images, accelerating voltage: 3 kV, working distance: 10 mm, probe current: 35, objective lens aperture: 3, secondary electrons capture duration: 80 s.

Immunohistochemical analysis of the Wnt signalling components in WT and DSPP-null mice

DSPP null mice and their matched wild type mice heads (post natal day3) were used for immunohistochemical analysis. Animal breeding and experimental procedures were approved and conducted in strict accordance with the guidelines and regulations stipulated by the Institutional Animal Care and Use committee at the University of Illinois at Chicago and in compliance with the ARRIVE (Animal Research: Reporting of in Vivo Experiments) guidelines. Formalin fixed paraffin-embedded specimen and paraffin block sectioning were conducted as described previously²⁹. Sections were treated with primary antibodies against Wnt5a/b, LRP5, LRP6, Frizzled5, Frizzled 6, and ROR2 (Rabbit mAb #88639). Sections were developed with VECTASTAIN® ABC HRP kit (Vector Laboratories,) (Vector Laboratories) as per manufacturer's protocol. The DAB Peroxidase (HRP) Substrate Kit (Vector Laboratories) was used for antigen detection. Sections were imaged with Carl Zeiss Axio Observer D1 inverted microscope. For fluorescence detection, an anti- β -catenin antibody, (Sigma,) was used, followed by Anti mouse-IgG Alexa 488 nm, then sections were counter stained with DAPI and mounted. Images were taken with a Zeiss 710 Meta Confocal Microscope at the UIC RRC Facility.

Statistical analysis

Data were presented as the mean \pm standard deviation of at least 3 independent experiments. Statistical significance of differences was calculated using the Student's t test. Significance of $p \leq 0.05$ was considered significant.

Data availability

Data Availability statements: The sequence data that support the findings of this study have been deposited in the GenBank repository with the accession number PP722978. The additional data that support the findings of this study are available from the corresponding author upon reasonable request.

Received: 18 March 2024; Accepted: 10 October 2024

Published online: 31 October 2024

References

- Goldberg, M., Kulkarni, A. B., Young, M. & Boskey, A. Dentin: structure, composition and mineralization. *Front. Biosci.* **3**, 711–735. <https://doi.org/10.2741/e281> (2011).
- Al Madhoun, A. et al. Dental pulp stem cells derived from adult human third molar tooth: a brief review. *Front. Cell. Dev. Biol.* **9**, 717624. <https://doi.org/10.3389/fcell.2021.717624> (2021).
- Xie, Z. et al. Functional dental pulp regeneration: basic research and clinical translation. *Int. J. Mol. Sci.* **22** <https://doi.org/10.3390/ijms22168991> (2021).
- Piva, E. et al. Dental pulp tissue regeneration using dental pulp stem cells isolated and expanded in human serum. *J. Endod.* **43**, 568–574. <https://doi.org/10.1016/j.joen.2016.11.018> (2017).
- Nijakowski, K., Ortarzewska, M., Jankowski, J., Lehmann, A. & Surdacka, A. The role of cellular metabolism in maintaining the function of the dentine-pulp complex: a narrative review. *Metabolites*. **13** <https://doi.org/10.3390/metabo13040520> (2023).
- Moradian-Oldak, J. & George, A. Biom mineralization of enamel and dentin mediated by matrix proteins. *J. Dent. Res.* **100**, 1020–1029. <https://doi.org/10.1177/00220345211018405> (2021).
- Ravindran, S. & George, A. Multifunctional ECM proteins in bone and teeth. *Exp. Cell Res.* **325**, 148–154. <https://doi.org/10.1016/j.yexcr.2014.01.018> (2014).
- George, A., Srinivasan, R., Thotakura, S. & Veis, A. The phosphophoryn gene family: identical domain structures at the carboxyl end. *Eur. J. Oral Sci.* **106**(Suppl 1), 221–226. <https://doi.org/10.1111/j.1600-0722.1998.tb02179.x> (1998).
- Zhang, Y. et al. DSPP contains an IRES element responsible for the translation of dentin phosphophoryn. *J. Dent. Res.* **93**, 155–161. <https://doi.org/10.1177/0022034513516631> (2014).
- He, G. et al. Phosphorylation of phosphophoryn is crucial for its function as a mediator of biomineralization. *J. Biol. Chem.* **280**, 33109–33114. <https://doi.org/10.1074/jbc.M500159200> (2005).
- Chen, Y., Zhang, Y., Ramachandran, A. & George, A. DSPP is essential for normal development of the dental-craniofacial complex. *J. Dent. Res.* **95**, 302–310. <https://doi.org/10.1177/0022034515610768> (2016).
- Verdelis, K. et al. DSPP effects on in vivo bone mineralization. *Bone*. **43**, 983–990. <https://doi.org/10.1016/j.bone.2008.08.110> (2008).
- Sreenath, T. et al. Dentin sialophosphoprotein knockout mouse teeth display widened predentin zone and develop defective dentin mineralization similar to human dentinogenesis imperfecta type III. *J. Biol. Chem.* **278**, 24874–24880. <https://doi.org/10.1074/jbc.M303908200> (2003).
- Eapen, A. & George, A. Dentin phosphophoryn in the matrix activates AKT and mTOR signaling pathway to promote preodontoblast survival and differentiation. *Front. Physiol.* **6**, 221. <https://doi.org/10.3389/fphys.2015.00221> (2015).
- Eapen, A. et al. Dentin phosphophoryn activates smad protein signaling through Ca²⁺-calmodulin-dependent protein kinase II in undifferentiated mesenchymal cells. *J. Biol. Chem.* **288**, 8585–8595. <https://doi.org/10.1074/jbc.M112.413997> (2013).
- Komiya, Y. & Habas, R. Wnt signal transduction pathways. *Organogenesis*. **4**, 68–75. <https://doi.org/10.4161/org.4.2.5851> (2008).
- Logan, C. Y. & Nusse, R. The Wnt signaling pathway in development and disease. *Annu. Rev. Cell Dev. Biol.* **20**, 781–810. <https://doi.org/10.1146/annurev.cellbio.20.010403.113126> (2004).
- Lin, M. et al. Wnt5a regulates growth, patterning, and odontoblast differentiation of developing mouse tooth. *Dev. Dyn.* **240**, 432–440. <https://doi.org/10.1002/dvdy.22550> (2011).
- Balic, A. & Thesleff, I. Tissue interactions regulating tooth development and renewal. *Curr. Top. Dev. Biol.* **115**, 157–186. <https://doi.org/10.1016/bs.ctdb.2015.07.006> (2015).
- Li, J., Parada, C. & Chai, Y. Cellular and molecular mechanisms of tooth root development. *Development (Cambridge England)* **144**, 374–384. <https://doi.org/10.1242/dev.137216> (2017).
- Hermans, F., Hemeryck, L., Lambrichts, I., Bronckaers, A. & Vankelecom, H. Intertwined signaling pathways governing tooth development: a give-and-take between canonical wnt and shh. *Front. Cell. Dev. Biol.* **9**, 758203. <https://doi.org/10.3389/fcell.2021.758203> (2021).
- Yu, M., Wong, S. W., Han, D. & Cai, T. Genetic analysis: wnt and other pathways in nonsyndromic tooth agenesis. *Oral Dis.* **25**, 646–651. <https://doi.org/10.1111/odi.12931> (2019).
- Duan, P. & Bonewald, L. F. The role of the wnt/ β -catenin signaling pathway in formation and maintenance of bone and teeth. *Int. J. Biochem. Cell Biol.* **77**, 23–29. <https://doi.org/10.1016/j.biocel.2016.05.015> (2016).
- Cai, J. et al. Wnt5a plays a crucial role in determining tooth size during murine tooth development. *Cell. Tissue Res.* **345**, 367–377. <https://doi.org/10.1007/s00441-011-1224-4> (2011).
- Sheng, R. et al. Cholesterol selectively activates canonical wnt signalling over non-canonical wnt signalling. *Nat. Commun.* **5**, 4393. <https://doi.org/10.1038/ncomms5393> (2014).
- Villasenor, T. et al. Activation of the wnt pathway by Mycobacterium tuberculosis: a wnt-wnt Situation. *Front. Immunol.* **8**, 50. <https://doi.org/10.3389/fimmu.2017.00050> (2017).
- Mikels, A. J. & Nusse, R. Purified Wnt5a protein activates or inhibits beta-catenin-TCF signaling depending on receptor context. *PLoS Biol.* **4**, e115. <https://doi.org/10.1371/journal.pbio.0040115> (2006).
- Bueno, M. L. P., Saad, S. T. O. & Roversi, F. M. WNT5A in tumor development and progression: a comprehensive review. *Biomed. Pharmacotherapy = Biomedicine Pharmacotherapie*. **155**, 113599. <https://doi.org/10.1016/j.biopha.2022.113599> (2022).
- Chen, Y., Pethö, A., Ganapathy, A. & George, A. DPP promotes odontogenic differentiation of DPSCs through NF- κ B signaling. *Sci. Rep.* **11**, 22076. <https://doi.org/10.1038/s41598-021-01359-3> (2021).
- Chen, F. E., Huang, D. B., Chen, Y. Q. & Ghosh, G. Crystal structure of p50/p65 heterodimer of transcription factor NF- κ B bound to DNA. *Nature*. **391**, 410–413. <https://doi.org/10.1038/34956> (1998).
- Okamoto, M. et al. Noncanonical Wnt5a enhances Wnt/ β -catenin signaling during osteoblastogenesis. *Sci. Rep.* **4**, 4493. <https://doi.org/10.1038/srep04493> (2014).

32. Trujano-Camacho, S. et al. Inhibition of Wnt- β -Catenin signaling by ICRT14 drug depends of post-transcriptional regulation by HOTAIR in human cervical cancer HeLa cells. *Front. Oncol.* **11**, 729228. <https://doi.org/10.3389/fonc.2021.729228> (2021).
33. Ruch, J. V. & Lesot, H. Bégue-Kirn, C. Odontoblast differentiation. *Int. J. Dev. Biol.* **39**, 51–68 (1995).
34. George, A. et al. The carboxyl-terminal domain of phosphophoryn contains unique extended triplet amino acid repeat sequences forming ordered carboxyl-phosphate interaction ridges that may be essential in the biomineralization process. *J. Biol. Chem.* **271**, 32869–32873. <https://doi.org/10.1074/jbc.271.51.32869> (1996).
35. Sabsay, B., Stetler-Stevenson, W. G., Lechner, J. H. & Veis, A. Domain structure and sequence distribution in dentin phosphophoryn. *Biochem. J.* **276**(Pt 3), 699–707. <https://doi.org/10.1042/bj2760699> (1991).
36. Kumawat, K. & Gosens, R. WNT-5A: signaling and functions in health and disease. *Cell. Mol. Life Sci.* **73**, 567–587. <https://doi.org/10.1007/s00018-015-2076-y> (2016).
37. Yamaguchi, T. P., Bradley, A., McMahon, A. P. & Jones, S. A Wnt5a pathway underlies outgrowth of multiple structures in the vertebrate embryo. *Development.* **126**, 1211–1223. <https://doi.org/10.1242/dev.126.6.1211> (1999).
38. Reynolds, K. et al. Wnt signaling in orofacial clefts: crosstalk, pathogenesis and models. *Dis. Models Mech.* **12**<https://doi.org/10.1242/dmm.037051> (2019).
39. He, F. et al. Wnt5a regulates directional cell migration and cell proliferation via Ror2-mediated noncanonical pathway in mammalian palate development. *Development.* **135**, 3871–3879. <https://doi.org/10.1242/dev.025767> (2008).
40. Sunohara, M., Morikawa, S., Asada, N. & Suzuki, K. Bimodal expression of Wnt5a in the tooth germ: a comparative study using in situ hybridization and immunohistochemistry. *Ann. Anat. - Anatomischer Anzeiger.* **240**, 151868. <https://doi.org/10.1016/j.aanat.2021.151868> (2022).
41. Suomalainen, M. & Thesleff, I. Patterns of wnt pathway activity in the mouse incisor indicate absence of Wnt/beta-catenin signaling in the epithelial stem cells. *Dev. Dyn.* **239**, 364–372. <https://doi.org/10.1002/dvdy.22106> (2010).
42. Hao, J., Ramachandran, A. & George, A. Temporal and spatial localization of the dentin matrix proteins during dentin biomineralization. *J. Histochem. Cytochem.* **57**, 227–237. <https://doi.org/10.1369/jhc.2008.952119> (2009).
43. Gross, J. C., Chaudhary, V., Bartscherer, K. & Boutros, M. Active wnt proteins are secreted on exosomes. *Nat. Cell. Biol.* **14**, 1036–1045. <https://doi.org/10.1038/ncb2574> (2012).
44. Dzialo, E. et al. WNT3a and WNT5a transported by exosomes activate WNT signaling pathways in human cardiac fibroblasts. *Int. J. Mol. Sci.* **20** <https://doi.org/10.3390/ijms20061436> (2019).
45. Ekström, E. J. et al. WNT5A induces release of exosomes containing pro-angiogenic and immunosuppressive factors from malignant melanoma cells. *Mol. Cancer.* **13**, 88. <https://doi.org/10.1186/1476-4598-13-88> (2014).
46. van Amerongen, R., Fuerer, C., Mizutani, M. & Nusse, R. Wnt5a can both activate and repress Wnt/ β -catenin signaling during mouse embryonic development. *Dev. Biol.* **369**, 101–114. <https://doi.org/10.1016/j.ydbio.2012.06.020> (2012).
47. Cantù, C. et al. A cytoplasmic role of Wnt/ β -catenin transcriptional cofactors Bcl9, Bcl9l, and Pygopus in tooth enamel formation. *Sci. Signal.* **10**<https://doi.org/10.1126/scisignal.aah4598> (2017).
48. Tokavanich, N., Wein, M. N., English, J. D., Ono, N. & Ono, W. The role of wnt signaling in postnatal tooth root development. *Front. Dent. Med.* **2**<https://doi.org/10.3389/fdmed.2021.769134> (2021).
49. Boland, G. M., Perkins, G., Hall, D. J. & Tuan, R. S. Wnt 3a promotes proliferation and suppresses osteogenic differentiation of adult human mesenchymal stem cells. *J. Cell. Biochem.* **93**, 1210–1230. <https://doi.org/10.1002/jcb.20284> (2004).
50. Gong, Y. et al. LDL receptor-related protein 5 (LRP5) affects bone accrual and eye development. *Cell.* **107**, 513–523. [https://doi.org/10.1016/s0092-8674\(01\)00571-2](https://doi.org/10.1016/s0092-8674(01)00571-2) (2001).
51. Li, T. et al. WNT5A interacts with FZD5 and LRP5 to regulate proliferation and self-renewal of endometrial mesenchymal stem-like cells. *Front. Cell. Dev. Biology.* **10**, 837827. <https://doi.org/10.3389/fcell.2022.837827> (2022).
52. Billiard, J. et al. The orphan receptor tyrosine kinase Ror2 modulates canonical wnt signaling in osteoblastic cells. *Mol. Endocrinol.* **19**(1), 90–101 (2005).
53. Schwabe, G. C. et al. Distinct mutations in the receptor tyrosine kinase gene ROR2 cause brachydactyly type B. *Am. J. Hum. Genet.* **67**, 822–831. <https://doi.org/10.1086/303084> (2000).
54. Schwabe, G. C. et al. Ror2 knockout mouse as a model for the developmental pathology of autosomal recessive Robinow syndrome. *Dev. Dyn.* **229**, 400–410. <https://doi.org/10.1002/dvdy.10466> (2004).
55. Ma, Y. et al. Ror2-mediated non-canonical wnt signaling regulates Cdc42 and cell proliferation during tooth root development. *Development.* **148**<https://doi.org/10.1242/dev.196360> (2021).
56. Yu, J. et al. Wnt5a induces ROR1/ROR2 heterooligomerization to enhance leukemia chemotaxis and proliferation. *J. Clin. Investig.* **126**, 585–598. <https://doi.org/10.1172/jci83535> (2016).
57. Xu, D., Mutoh, N., Ohshima, H. & Tani-Ishii, N. The effect of mineral trioxide aggregate on dental pulp healing in the infected pulp by direct pulp capping. *Dent. Mater. J.* **40**, 1373–1379. <https://doi.org/10.4012/dmj.2020-393> (2021).
58. Liu, Y., Rubin, B., Bodine, P. V. & Billiard, J. Wnt5a induces homodimerization and activation of Ror2 receptor tyrosine kinase. *J. Cell. Biochem.* **105**, 497–502. <https://doi.org/10.1002/jcb.21848> (2008).
59. Sui, B. et al. Dental pulp stem cells: from discovery to clinical application. *J. Endod.* **46**, S46–S55. <https://doi.org/10.1016/j.joen.2020.06.027> (2020).
60. Jenei, V. et al. A t-butyloxycarbonyl-modified Wnt5a-derived hexapeptide functions as a potent antagonist of Wnt5a-dependent melanoma cell invasion. *Proc. Natl. Acad. Sci. U S A.* **106**, 19473–19478. <https://doi.org/10.1073/pnas.0909409106> (2009).
61. Ramachandran, A. et al. TRIP-1 in the extracellular matrix promotes nucleation of calcium phosphate polymorphs. *Connect. Tissue Res.* **59**, 13–19. <https://doi.org/10.1080/03008207.2018.1424146> (2018).
62. Tao, Y. et al. Tailored tetravalent antibodies potently and specifically activate Wnt/Frizzled pathways in cells, organoids and mice. *eLife.* **8**, e46134. <https://doi.org/10.7554/eLife.46134> (2019).

Acknowledgements

We thank Dr. Karen Katula, University of N. Carolina, Greensboro for the Wnt5a promoter construct and Dr. Lyndon Cooper, Virginia Commonwealth University, Virginia for NF- κ B RE promoter construct and Dr. Sezar Seshagiri (AntlerA Therapeutics, Inc.) for pF-panFZD5/6-L6=LRP antibody. This study was supported by grants from the National Institutes of Health R01 DE028531 and R01 DE031737 and the Brodie Endowment Fund.

The funders had no role in study design, data collection, and interpretation, or the decision to submit the work for publication.

Author contributions

Y.C. performed ChIP analysis, CRISPR gene editing, cell proliferation and differentiation analysis, RT-PCR and Western blotting, IHC, confocal image analysis, data analysis and wrote the manuscript. A.P. performed RT-PCR and Western Blotting. A.Ga. performed cell proliferation analysis; A.Ge. designed the research and wrote and edited the final manuscript, and obtained the financial support. The manuscript has been read and approved by

all the authors.

Declarations

Competing interests

The authors declare no competing interests.

Additional information

Supplementary Information The online version contains supplementary material available at <https://doi.org/10.1038/s41598-024-76069-7>.

Correspondence and requests for materials should be addressed to A.G.

Reprints and permissions information is available at www.nature.com/reprints.

Publisher's note Springer Nature remains neutral with regard to jurisdictional claims in published maps and institutional affiliations.

Open Access This article is licensed under a Creative Commons Attribution-NonCommercial-NoDerivatives 4.0 International License, which permits any non-commercial use, sharing, distribution and reproduction in any medium or format, as long as you give appropriate credit to the original author(s) and the source, provide a link to the Creative Commons licence, and indicate if you modified the licensed material. You do not have permission under this licence to share adapted material derived from this article or parts of it. The images or other third party material in this article are included in the article's Creative Commons licence, unless indicated otherwise in a credit line to the material. If material is not included in the article's Creative Commons licence and your intended use is not permitted by statutory regulation or exceeds the permitted use, you will need to obtain permission directly from the copyright holder. To view a copy of this licence, visit <http://creativecommons.org/licenses/by-nc-nd/4.0/>.

© The Author(s) 2024